UNIVERSITY OF SZEGED
Faculty of Science and Informatics

DOCTORAL THESIS

Whole cell patch clamp analysis of non-synaptic and synaptic signaling in rodent and human supragranular neocortex

Author:
Márton RÓZSA

Supervisor:
Prof. Gábor TAMÁS

MTA-SZTE Research Group for Cortical Microcircuits
Department of Physiology, Anatomy and Neuroscience

2018
Szeged

Contents

List of Figures

List of Abbreviations

AAC	**a**xo-**a**xonic **c**ell
ABC	**c**onjugated **a**vidin-**b**iotin horseradish peroxidase
AHP	spike **a**fter **h**yper**p**olarization
AZ	**a**ctive **z**one
BC	**b**asket **c**ell
BDA	**b**iotinylated **d**extran **a**mine
$[Ca^{2+}]_o$	extracellular calcium ion concentration
D-AP-5	**D**-2-**a**mino-5-**p**hosphonopentanoate
DAB	3,3′-**dia**mino**b**enzidine
eX	**e**mbryonic day X
EM	**e**lectron **m**icroscopy
EPSC	**e**xcitatory **p**ost**s**ynaptic **c**urrent
EPSP	**e**xcitatory **p**ost**s**ynaptic **p**otential
GABA	γ-**a**mino**b**utyric **a**cid
GIRK	**G**-protein gated **i**nwardly **r**ectifying potassium channel
GMM	**g**aussian **m**ixture **m**odels
IN	**i**nter**n**euron
KIR	**i**nwardly **r**ectifying potassium channel
LM	**l**ight **m**icroscopy
MPFA	**m**ultiple **p**robability **f**luctuation **a**nalysis

MVR	**m**ulti**v**esicular **r**elease
NGFC	**n**euro**g**lia**f**orm **c**ell
NG2	**n**euron-**g**lial antigen **2**
NMDA	**N**-**M**ethyl-**D**-**a**spartate
MW U-test	**M**ann **W**hitney **U**-test
W SR-test	**W**ilcoxon **s**igned **r**ank-test
N_{FRS}	**n**umber of **f**unctional **r**elease **s**ites
N_{LM}	**n**umber of putative synapses based on **l**ight **m**icroscopy
OGB-1	**O**regon **G**reen **B**APTA-1
PB	**p**hosphate **b**uffer
PC	**p**yramidal **c**ell
Pr	**p**robability of **r**elease
PSD	**p**ost**s**ynaptic **d**ensity
pX	**p**ostnatal day X
q	**q**uantal size
R_A	**a**ccess **r**esistance
R_{In}	**in**put **r**esistance
R_{SUM}	**sum**med **r**esistance
ROI	**r**egion **o**f **i**nterest
SD	**s**tandard **d**eviation
TBS	**t**ris-**b**uffered **s**aline

1 Introduction

The neocortex is the evolutionarily youngest part of the cerebral cortex and considered one of the most complex biological structures. Besides its crucial role in brain functions such as sensory perception and motor execution, it gives us a capacity for sophisticated cognitive tasks (Roth and Dicke, 2005). These cognitive abilities make neuroscientists so eager –and able– to decipher the workings of the human brain. Although the ultimate goal in neuroscience is to answer the question "how the human brain operates", most of the cellular neuroscience research is currently focusing on understanding the nervous system of simpler and more available model organisms, such as rodents'. Despite the fact that plenty of data exist from these model organisms, it still proves to be quite ambitious a task (Markram et al., 2015). Thus, overall, there are at least two straightforward ways to propel current neuroscience research: either to unveil the fine details of the rodent brain or to use this knowledge and collide these results with research done in the human brain. In my doctoral study, we have followed each paths. First, we characterize a novel communication pathway from identified GABAergic interneuron types to astrocyte glia cells. Second, we demonstrated a species-specific difference in a well known synaptic pathway between the human and rodent neocortex.

1.1 Neocortical neurons

The cortical neurons can be divided in two main groups: the excitatory projecting pyramidal cells (McCormick et al., 1985) and the inhibitory local interneurons (Peters, Saint Marie, and Peters E. G., 1984). The pyramidal cells and other glutamatergic neuron types comprise the majority of the neocortical neurons, approximately 80–90%, (Tremblay, Lee, and Rudy, 2016). There are multiple subtypes of cortical pyramidal cells differing in their morphology, gene expression and projection profile (Spruston, 2008; Tasic et al., 2017). The pyramidal cell subtypes are arranged in layers giving the neocortex its typical laminar architecture. Their common characteristic features are the spiny dendrites, a triangular cell body, a set of basal dendrites and a thick, radially oriented apical dendrite which usually forms a terminal tuft in the superficial cortical layers. In general, pyramidal cells are responsible for the majority of excitatory glutamatergic postsynaptic synapses in the neocortex. Pyramidal cells mainly innervate dendritic spines of other pyramidal cells and dendritic shafts of aspiny interneurons.

GABAergic interneurons constitute the minor fraction of neurons in the neocortex (10–20%) but are instrumental for normal brain function (Tremblay, Lee, and Rudy, 2016). Despite their relative scarcity, these interneurons display extremely diverse morphological, electrophysiological and molecular properties and, therefore, it was always tempting for neuroscientist to classify them on the basis of these characteristics (Cauli et al., 1997; DeFelipe, 1993; Gupta, Wang, and Markram, 2000; Kawaguchi and Kubota, 1997; Kepecs and Fishell, 2014; Tasic et al., 2016; Tasic et al., 2017). The recent advent of high-throughput transcriptomic single cell profiling has enabled neuroscientist to classify neocortical neurons in a robust, scalable and unbiased way. (Tasic et al., 2016; Tasic et al., 2017; Zeisel et al., 2015). Although

these results are still nascent, they are in line with earlier studies that report correlating electrophysiological, anatomical and molecular cell types (Gupta, Wang, and Markram, 2000; Kawaguchi, 1993; Kawaguchi and Kubota, 1996; Kawaguchi and Kubota, 1997; Kepecs and Fishell, 2014).

The most ubiquitous member of the GABAergic cells is the basket cell type representing nearly 50 % of the GABAergic neurons in the neocortex (Markram et al., 2004). The name "basket cell" was first used by Ramón y Cajal for a specific nerve cell type in the cerebellum. Axon terminals initiating from these neurons surround the somata of large Purkinje cells, creating „basket-like structures" around their cell bodies. Hence, GABAergic interneurons in all brain regions that form a high fraction of axo-somatic synapses have, therefore, traditionally been classified as basket cells (Freund and Katona, 2007; Hendry and Jones, 1985; Kisvárday, Beaulieu, and Eysel, 1993; Somogyi et al., 1983) and thus basket cells are a heterogeneous population (Tasic et al., 2016; Tasic et al., 2017).

On the other hand axo-axonic cell comprise a unique and homogeneous class of cortical interneurons (Somogyi et al., 1998; Tasic et al., 2016; Tasic et al., 2017). These cells selectively innervate nearby pyramidal cells and exclusively target their axon initial segments (Somogyi, 1977). Axo-axonic interneurons elicit fast GABAergic currents on their target cells providing direct inhibition to the generation site of the action potentials (Buhl et al., 1994; Maccaferri et al., 2000; Pawelzik et al., 1999). However, the function of axo-axonic cells in cortical circuits is debated due to the fact that in certain conditions these cells can provide excitation of the target pyramidal cells though depolarizing GABAergic potential in the axon initial segment (Molnár et al., 2008; Szabadics et al., 2006; Woodruff et al., 2009; Woodruff et al., 2011).

Basket and axo-axonic cells share some common features such as expression of

parvalbumin (a cytoplasmic calcium-binding protein) and short action potential duration associated with fast maximal firing frequency. Hence, they are often called fast-spiking interneurons. Furthermore, both basket and axo-axonic cells are known for being heavily innervated by local pyramidal cells and for their membranes with fast time constant. These mean that excitatory synaptic inputs can efficiently and reliably trigger action potentials in them (Fricker and Miles, 2000; Galarreta and Hestrin, 2001; Szegedi et al., 2017). These interneurons in turn can effectively regulate the action potential generation of surrounding pyramidal cells with their GABAergic axon terminals targeting the somatic region or axon initial segment of nearby pyramidal cells.

According to the classical interpretation, the output of individual GABAergic interneurons –including basket and axo-axonic cells– in the cerebral cortex is mediated via synapses operating in a spatially and temporally highly regulated manner (Freund and Buzsáki, 1996; Klausberger and Somogyi, 2008; Markram et al., 2004; Miles and Wong, 1984; Pouille and Scanziani, 2004; Thomson et al., 2002). Apart from targeting receptors located in the postsynaptic density, the synaptically released GABA can diffuse out of the synaptic cleft to reach extrasynaptic receptors producing tonic inhibition (Barbour and Häusser, 1997; Farrant and Nusser, 2005; Otis, Staley, and Mody, 1991). A unique type of GABAergic inhibitory interneuron, neurogliaform cell (NGFC), has specialized in acting on GABA receptors on compartments of the neuronal surface which do not receive synaptic junctions. A NGFC forms an extremely dense local axonal cloud with GABA-releasing boutons and with a single action potential can flood the extracellular space with GABA through a unitary form of volume transmission (Agnati et al., 2006; Capogna and Pearce, 2011; Oláh et al., 2009; Overstreet-Wadiche and McBain, 2015; Vizi, Kiss, and Lendvai, 2004). The GABA released by a single action potential can effectively reach the extrasynaptic

$GABA_A$ and $GABA_B$ receptors on virtually all neuronal processes within the extremely dense axonal cloud of the NGFC (Capogna and Pearce, 2011; Oláh et al., 2007; Oláh et al., 2009). In the same vein, neurogliaform interneurons might act on non-neuronal elements of the surrounding cortical tissue without establishing synaptic contacts.

1.2 Glia in the neocortex

Glial cells are the major class of non-neuronal cells in the brain (Butt and Verkhratsky, 2013). Their diversity and complex role have been overlooked in the dawn of neuroscience. They were regarded as connective tissue with relatively simple structural function, hence their name (the Greek word γλια refers to glue or glutinous substance). Yet, glial cells have become the focus of scientific attention in the last decades. According to modern textbooks, glial cells comprise two main groups: microglia with mesodermal origin and macroglia with ectodermal origin. The macroglia group in the central nervous system consists of three subgroups with distinctive morphology, function and gene expression profile: oligodendrocytes, NG2-glia and astrocytes (Cahoy et al., 2008; Tasic et al., 2016; Tasic et al., 2017; Zhang et al., 2014). Despite their different origin and multitude of roles, the ultimate goal of neuroglia is to support the neuronal function (Butt and Verkhratsky, 2013): microglia represent the innate brain immunity and defense, oligodendrocytes myelinate and thus insulate the neuronal axons, NG2-glia act as precursor cells, and astrocytes are the main homeostatic cells of the gray matter with multiple functions.

1.2.1 Developmentally regulated roles of astrocytes

Astrocytes are extensively studied due to the fact that they comprise the most abundant and diverse glia class (Matyash and Kettenmann, 2010; Zhang and Barres, 2010). In general all mature astrocytes share the same basic functions: they are crucial for the extracellular ionic homeostasis, neurotransmitter uptake, synapse formation and regulation of blood–brain-barrier (Butt and Verkhratsky, 2013). During the course of development astrocytes have changing functions. Immature astrocytes are generated by the neuronal progenitor cells in the subventricular zone. They migrate into the cortex and undergo symmetric divisions. The overall proliferation of astrocytes takes place roughly between e18 (embryonic day 18) and p14 (postnatal day 14) (Ge et al., 2012; Sauvageot and Stiles, 2002). Until they acquire their mature form and functions, astrocytes participate in the developmental synaptogenesis, during which the number of synapses dramatic increases in the brain (Freeman, 2010). The major waves of rodent CNS synaptogenesis occur roughly around p15 to p25 (De Felipe et al., 1997; Lund and Lund, 1972; Warton and McCart, 1989). This is the time when astrocytes grow and differentiate (Bushong, Martone, and Ellisman, 2004). The maturation of astrocytic morphology goes hand-in-hand with a change in their electrophysiological properties, protein and gene expression profiles (Cahoy et al., 2008; Meier, Kafitz, and Rose, 2008; Sun et al., 2013; Zhou, 2005). By postnatal day 30 (after the major wave of synapse formation), astrocytes have taken on their mature morphology, electrophysiology, gene and receptor expression profiles: they occupy unique spatial domains (Bushong et al., 2002; Ogata and Kosaka, 2002) engulfing synapses within their territory with fine and elaborated filopodial processes (Bushong, Martone, and Ellisman, 2004; Freeman, 2010). In addition, their membrane potential is highly negative (resting membrane potential is roughly between

-80 and –90 mV) and their membrane is electrophysiologically leaky due to high permeability for potassium ions (Mishima and Hirase, 2010; Zhou, 2005). Furthermore, the receptors and ion channels they express is typical to astrocytes in the adult brain (Cahoy et al., 2008; Meier, Kafitz, and Rose, 2008; Sun et al., 2013).

1.3 GABAergic neuron-to-glia communication

Direct synaptic junctions from neurons to non-neuronal cells appear to be restricted to connections linking neurons and NG2-expressing glial cells (Bergles et al., 2000; Lin and Bergles, 2004; Maldonado and Angulo, 2015) in the cerebral cortex. In spite of the apparent absence of synapses on other glial cells, the presence of GABA receptors and transporters is well established (Eulenburg and Gomeza, 2010; Porter and McCarthy, 1997), and depolarizing GABAergic responses are characteristic of glia (Kettenmann, Backus, and Schachner, 1984). Accordingly, potentially non-synaptic GABAergic interactions between neurons and glia have been suggested by exogenously applied agonists (Kettenmann, Backus, and Schachner, 1984; Meier, Kafitz, and Rose, 2008) or prolonged, high-frequency stimulation of GABAergic interneurons (Covelo and Araque, 2018; Egawa et al., 2013; Kaila et al., 1997; Kang et al., 1998; Mariotti et al., 2018; Perea et al., 2016). However, evidence for GABA-evoked astrocyte activation by physiological activity processes is lacking. (Losi, Mariotti, and Carmignoto, 2014; Vélez-Fort, Audinat, and Angulo, 2012).

1.4 Unique features of the human neocortex

In the past decade, increasing attention has been put on special features of the human neocortex microcircuits comparing them to those of other mammals such as non-human primates, carnivores, and rodents (Boldog et al., 2017; Komlósi et al.,

2012; Mohan et al., 2015; Molnár et al., 2008; Oláh et al., 2007; Prince and Wong, 1981; Schwartzkroin and Knowles, 1984; Verhoog et al., 2013; Wang et al., 2015; Yáñez et al., 2005). Species-specific differences evidently exist in various anatomical features of the neocortex including the layering, some long-range connections and some intrinsic electrical and morphological properties of nerve cells (Boldog et al., 2017; Mohan et al., 2015; Wang et al., 2015). Yet,it has been thought that basic cellular elements and local synaptic circuits are fairly stereotyped among mammalian species and largely similar for instance between a rodent and a human. Supporting the idea, cortical GABAergic interneuron types with similar basic features have been characterized in the rodent and the human neocortex. In addition, numerous pyramidal cell features and local synaptic connectivity patterns were reported to be largely similar in the rodent and in the human (Komlósi et al., 2012; Molnár et al., 2008; Oláh et al., 2007; Yáñez et al., 2005). However, classic theories suggest that synaptic properties also contribute to cognitive abilities (Bliss and Gardner-Medwin, 1973; Buzsáki, 2015; Hebb, 1949; Singer, 1995) and recent studies revealed differences in synaptic communication between cell types that are highly conserved among mammals. Human cortical pyramidal cell to pyramidal cell connections display spike timing-dependent long-term plasticity similar to that found in rodents, but with slightly different activity patterns for plasticity induction (Verhoog et al., 2013). It has also been demonstrated that the synaptic outputs of individual human pyramidal cells can be very powerful. In fact, some human layer 2/3 pyramidal cell contacts to GABAergic interneurons are so powerful that individual presynaptic action potentials result in suprathreshold postsynaptic responses in GABAergic neurons. This in turn triggers polysynaptic series of events downstream in the network (Komlósi et al., 2012; Molnár et al., 2008; Szegedi et al., 2016; Szegedi et al.,

2017). Such powerful synaptic connections between pyramidal cells and interneurons have not been reported in rodent neocortex (Jiang et al., 2015; Miles and Wong, 1986). These specific features were speculated to represent an evolutionary adaptation to the human brain indicating that they might be important for information processing in the human neocortex (Woodruff and Yuste, 2008).

2 Aims

This thesis has two aims: 1) to elucidate the effect of GABA released by unitary volume transmission from a neocortical neurogliaform interneurons to astrocytes. 2) to study specific differences of a highly conserved synaptic pathway, the excitatory connections from pyramidal cells to basket and axo-axonic interneurons in the rat and the human neocortex. Our specific questions were the following:

1. Does physiological spiking activity (e.g. single action potential) of an interneuron elicit the GABA-mediated currents in astrocytes? In addition, are there differences between interneuron types (neurogliaform cell versus non-neurogliaform cell) in their capacity to elicit the currents/potentials?

2. If so, what cellular level mechanisms are involved in the GABAergic astrocytic currents?

3. Is the physiologically released GABAergic response in astrocytes associated with cytoplasmic calcium transients?

4. How biophysical and structural features differ between excitatory glutamatergic synapses from a pyramidal cell to fast spiking interneuron in the rodent and human neocortex?

3 Author contributions

In the interneuron-astrocyte coupling study, the electrophysiological and imaging experiments and the analysis of the data performed was performed by me, Dr. Judith Baka performed the *post hoc* anatomical work and analysis, me together with Sándor Bordé wrote the scripts for cell clustering based on their electrophysiological features, Dr. Balázs Rózsa and Dr. Gergely Katona built the two-photon microscope.

In the human study, Prof. Pál Barzó provided us the human tissue samples, me and Dr. Gábor Molnár acquired the electrophysiology data, Dr. Judith Baka performed the *post hoc* anatomical work together with Dr. Noémi Holderith.

Prof. Gábor Tamás and Prof. Zoltán Nusser concieved the projects and helped in designing the experiments.

4 Materials and Methods

All procedures were performed according to the Declaration of Helsinki with the aproval of the University of Szeged Ethical Committee.

4.1 Slice preparation

4.1.1 Rodent brain slice preparation

Experiments were conducted according to the guidelines of the University of Szeged Animal Care and Use Committee. Astrocytes are considered mature after postnatal day 20 (p20) (Bushong, Martone, and Ellisman, 2004; Cahoy et al., 2008; Sun et al., 2013; Zhou, 2005); thus, for the experiments including astrocytes we used somatosensory cortex of young adult (p25–46, p37.4 $\pm$ 4.5, n = 137) male Wistar rats. In the experiments studying synaptic input to fast spiking interneurons, we used somatosensory cortex of male Wistar rats (p18–28, n = 9) and medial prefrontal cortex of adult male Wistar rats (p53–65, n = 8).

Animals were anaesthetized using volatile anesthetics halothane. Following decapitation, the brain was removed and immediately put in an ice-cold cutting solution composed of (in mM) 85 NaCl, 3 KCl, 1 NaH_2PO_4, 24 $NaHCO_3$, 0.5 $CaCl_2$, 4 $MgSO_4$, 25 D(+)-glucose, 75 sucrose. The solution was continuously gassed with 95 % O_2, and 5 % CO_2. After the removal of the brain, coronal slices (350 µm thick) were cut using a vibrating blade microtome (Microm HM 650 V) perpendicular to

cortical layers from the somatosensory or the medial prefrontal cortex. Next, slices were incubated at room temperature for 1 h in a solution composed of (in mM) 130 NaCl, 4.5 KCl, 1 NaH_2PO_4, 24 $NaHCO_3$, 1 $CaCl_2$, 3 $MgSO_4$, 10 D(+)-glucose, gassed with mixture of 95 % O_2, and 5 % CO_2.

4.1.2 Human brain slice preparation

Human slices were derived from material that had to be removed to gain access for surgical treatment of deep-brain tumors in left or right frontal (n = 22), temporal (n = 14), and parietal (n = 3) regions with written informed consent of female (n = 15, aged 53 $\pm$ 13 years) and male (n = 11, aged 43 $\pm$ 24 years) patients prior to surgery.

Anesthesia was induced with intravenous midazolam and fentanyl (0.03 mg/kg, 1–2 mg/kg, respectively). In addition, a bolus dose of propofol (1–2 mg/kg) was administered intravenously. To facilitate endotracheal intubation, the patient received 0.5 mg/kg rocuronium. The trachea was intubated and the patient was ventilated with a mixture of O_2 and N_2O at a ratio of 1:2. Anaesthesia was maintained with sevoflurane at monitored anaesthesia care volume of 1.2–1.5. After surgical removal of tissue blocks, they were immediately immersed in ice-cold cutting solution whereupon slices were resected and incubated in the same way as the rodent tissue.

4.2 Electrophysiology

The solution used for recordings had the same composition as the incubating solution except that the concentrations of $CaCl_2$ and $MgSO_4$ were 3 mM and 1.5 mM, respectively. Given that neurons and mature astrocytes have similar intracellular ionic milieux (Ballanyi, Grafe, and Bruggencate, 1987; Ma, Xie, and Zhou, 2012), we used the same intracellular solution for both. The micropipettes (3–6 MΩ) were filled

with (in mM) 126 K-gluconate, 4 KCl, 4 ATP-Mg, 0.3 GTP-Na_2, 10 HEPES, 10 creatin phosphate (pH 7.25; 300 mOsm). For presynaptic PCs, the intracellular solution contained in addition 10 mM L-glutamic acid (and correspondingly only 116 mM K-gluconate) to prevent the rundown of postsynaptic responses (Biró, Holderith, and Nusser, 2005; Ishikawa, Sahara, and Takahashi, 2002). To reveal anatomy of the recorded neurons we added 8 mM biocytin in the filling solution. In recordings from astrocytes, we used 0.3 mM biotinylated dextran (BDA) in order to avoid extensive dye coupling between cells through gap junctions. For some experiments, 1 mM GDP-β-S was added in the filling solution.

Somatic whole-cell recordings were obtained at 36 °C from simultaneously recorded doublets of interneurons and astrocytes or doublets pyramidal cells and fast spiking interneurons visualized with infrared differential interference contrast videomicroscopy (Olympus BX microscopes equipped with oblique illumination, Luigs & Neumann Infrapatch setup and HEKA EPC 10 USB patch-clamp amplifier). Signals were filtered at 7 kHz, digitized at 20-100kHz, and analyzed with Patchmaster (HEKA) and MATLAB (The MathWorks) softwares. Presynaptic interneurons and pyramidal cells were triggered to deliver action potentials with brief (1–20 ms) depolarizing suprathreshold pulses in current clamp mode at intervals >90 s and 5 s (in recordings from interneurons-astrocyte pairs and pyramidal cell interneuron pairs, respectively).

4.2.1 Astrocytic recording and pharmacology

The postsynaptic astrocytes were recorded in voltage clamp mode in order to optimize signal-to-noise ratio. The astrocytes were held at their resting membrane potential which was determined in current clamp mode with zero holding current. The average astrocytic membrane potential was -90.2 $\pm$ 3.9 mV, close to the calculated

equilibrium potential (–89 mV) for potassium ions. Astrocytes cannot be perfectly clamped from the somata due to their elaborate processes and exceptionally low input resistance; thus, the recorded currents might reflect the activity taking place relatively close to the tip of the recording electrode.

The astrocytic access resistance (R_A) was measured in voltage clamp mode by applying a voltage step (–5 mV, 100 ms) and measuring the initial peak current and calculating the resistance from Ohm's law. The astrocytic input resistance (R_{In}) estimation consisted of two steps. First, we determined the sum of the input and access resistance ($R_{SUM} = R_A + R_{In}$) in current clamp mode (without bridge balancing) by measuring steady-state voltage deflection in response to a hyperpolarizing current step (–200 pA, 800 ms). Next, we measured access resistance in voltage clamp mode as described above. The input resistance (R_{In}) was calculated as R_{SUM} - R_A.

All experiments studying effects of pharmacological agents in NGFC-astrocyte pairs were carried out eliciting single presynaptic action potentials. Experiments were discarded if astrocye access resistance exceeded 25 MΩ or changed more than 25 % during experiment. CGP35348 was applied in 40 µM concentration and purchased from Tocris; gabazine, NO-711 and GDP-β-S were applied in 5, 100 µM, and 1 mM, respectively, and were purchased from Sigma-Aldrich.

4.2.2 Recording for multiple probability fluctuation analysis

For multiple probability fluctuation analysis (MPFA) the access resistance (R_A) and whole-cell capacitance of the postsynaptic interneurons (IN) were continuously monitored during experiments. The R_A was 19.7 ± 6.9 MΩ and after series resistance compensation (66–73%) reduced to 6.0 ± 2.2 MΩ. Experiment was discarded if the compensated R_A reached 120% of the initial value during the recording. The postsynaptic cell membrane potential was voltage clamped at –70 mV. Stability of the

evoked peak amplitudes throughout a recording condition was determined by fitting the amplitude-time relationship with a linear function and assessing its slope. Recording epochs with slope < 0.01 pA s^{-1} in absolute value were considered stable. Elapsed time from tissue removal until the start of MPFA experiment was 9.8 ± 4.1 h (n = 10) 5.3 ± 1.8 h (n = 12) for the human and rat samples, respectively. For comparison of the MPFA experiments (in which extracellular Ca^{2+} and Mg^{2+} concentration was sequentially altered), we performed control experiments with standard calcium concentration to monitor possible rundown of EPSCs during long-lasting paired recordings. We studied pyramidal cell to basket cell pairs (n = 5) and the recordings lasted from 50 min up to 90 min. Yet, we found no significant decrease in the amplitude or charge between epochs selected from the early and late part of recordings (50 traces, charge: $p > 0.41$; amplitude: $p > 0.21$, unpaired t-test)

The multiple probability fluctuation analysis (MPFA) was performed by sequentially altering extracellular Ca^{2+} and Mg^{2+} ion concentrations in three to five different conditions (Biró, Holderith, and Nusser, 2005; Silver, Momiyama, and Cull-Candy, 1998; Silver, 2003). The ionic concentrations were changed from lower to higher Ca^{2+} concentrations and adding the following compounds to the extracellular solution: 20 mM DL - 2 - Amino - 5 - phosphonopentanoic acid (AP-5) (Tocris), 10 mM 1 - (2 , 4 - Dichlorophenyl) - 5 - (4 - iodophenyl) - 4 - methyl - N - 1 - piperidinyl - 1H - pyrazole - 3 - carboxamide (AM251) (Sigma-Aldrich), 0.5 mM γ-D-glutamylglycine (γDGG) (Abcam). On average 73 and 78 events were used for the MPFA in each condition in human and rat, respectively.

4.3 Two-photon calcium imaging

Astrocytes were filled with two fluorescent dyes: a Ca^{2+}-insensitive fluorophore (Alexa Fluor 594, 20–50 µM, Invitrogen), and a Ca^{2+}-sensitive fluorophore (Oregon Green BAPTA-1, 120 µM, Invitrogen). Red fluorescence was used to identify glial processes and cancel movement artefacts. In addition, neurons were occasionally filled with Alexa Fluor 594 (20–50 µM). Imaging was performed with a Femto3D-AO (Femtonics Ltd.) acousto-optic laser-scanning microscope (Katona et al., 2012) driven by a MaiTai femtosecond pulsing laser (MaiTai, SpectraPhysics) tuned to 850 nm wavelength. We used a 60× Olympus (NA = 0.9) objective in order to resolve small processes. Both reflected and transmitted fluorescent lights were collected (through an oil-immersion condenser, Olympus; numerical aperture, NA = 1.4). From 150 to 500 regions of interest (ROIs) were automatically selected in an approximately $100 \times 100 \times 50$ µm volume based on previously obtained Z-stacks. Image acquisition was controlled by custom-made software written in MATLAB (MES, Femtonics Ltd.). In the 60–120 second-long imaging sessions, sampling frequency for each ROI ranged from 40 to 120 Hz, with 3–8 mW laser power on the slice during the imaging.

4.4 *Post hoc* anatomical analysis

4.4.1 Histology and light microscopy

The electrophysiologically recorded cells were filled with biocytin or biotinylated dextran, which allowed *post hoc* anatomical analysis of the studied cells and their connections. Following electrophysiological recordings, slices were fixed in a solution containing 4 % paraformaldehyde, 15 % picric acid and 1.25 % glutaraldehyde

in 0.1 M phosphate buffer (PB; pH = 7.4) at 4 °C for at least 12 h. After several washes in 0.1 M PB, slices were cryoprotected in 10 % then 20 % sucrose solution in 0.1 M PB. Slices were swiftly frozen in liquid nitrogen then thawed in PB, whereupon they were embedded in 10 % gelatin and further re-sectioned into slices of 60 µm in thickness. The sections were incubated in a solution of conjugated avidin-biotin horseradish peroxidase (ABC; 1:100; Vector Labs) in Tris-buffered saline (TBS, pH = 7.4) at 4 °C overnight. The enzyme reaction was revealed by 3'3-diaminobenzidine tetrahydrochloride (0.05 % , DAB) as a chromogen and 0.01 % H_2O_2 as an oxidant. Then, sections were post fixed with 1 % OsO_4 in 0.1 MPB. After several washes in distilled water, they were stained in 1 % uranyl acetate, and finally dehydrated in ascending series of ethanol. The sections were infiltrated with epoxy resin (Durcupan) overnight and embedded on glass slices. Three dimensional light microscopic reconstructions were carried out using Neurolucida system with 100× objective. In genera, anatomical recovery rates were lower than expected in the case of interneuron-astrocyte pairs. We kept recording NGFC–astrocyte pairs in each recording paradigm until we had at least two NGFCs anatomically recovered. NGFCs were identified by their relatively small soma, dense local axonal arborization, and thin axons bearing a large number of boutons. On the contrary, the non-NGFCs studied here had relatively large somata and sparse axonal arborization, and their axon usually reached other cortical layers as well.

4.4.2 Electron microscopy

Visualization of biocytin and correlated light and electron microscopy (LM and EM) were performed as described previously (Oláh et al., 2009; Szabadics et al., 2006). Dendritic segments (distance from the soma ~50 µm in rat and ~150 µm in human)

of biocytin filled basket cells were re-embedded and re-sectioned at 20 nm thickness. Basket cells were identified by their distinctive electrophysiological properties and LM investigation of their characteristic axonal arbor. Digital images of serial EM sections were taken at 64000× magnification with a FEI/Philips CM10 electron microscope equipped with a MegaView G2 camera. Dendrites and presynaptic boutons were 3D-reconstructed using the Reconstruct software. The active zone areas were measured at perpendicularly cut synapses, where the rigid apposition of the pre- and postsynaptic membranes was clearly visible, and the docked vesicles were identified as described previously (Holderith et al., 2012). Active zones were identified by the parallel rigid membrane appositions where the synaptic cleft widened (because the postsynaptic density (PSD) is masked by dark DAB precipitate). Potential inhibitory synapses with flattened vesicles were discarded from the analysis. Bouton volumes of a subpopulation of boutons were measured from 20 nm thick serial reconstructions where the series contained the entire terminal (n = 9 human boutons, n = 8 rat boutons). We calculated the volume of the same subset of boutons from the area of the largest cross-section (assuming that boutons are spherical) and found a tight correlation (r = 0.9019, Spearman correlation) with the measured volume. Based on this correlation, we calculated the volume from the largest cross-section of those terminals where the AZ was measured but the series did not contain the entire terminal.

4.5 Data analysis and statistics

The analysis of the astrocyte electrophysiology and imaging data were performed using MATLAB software with Statistics Toolbox, Image Processing Toolbox, and custom written scripts. Data obtained from the pyramidal cell-to-interneuron pairs

were analyzed with Fitmaster (HEKA), Origin 7.5 (OriginLab), and Igor Pro (Wavemetrics) programs.

4.5.1 Astrocytic currents

For measurement of the early and the late component of the NGFC-evoked current in astrocytes, traces were downsampled to 1 kHz and a moving average was applied to the traces (5 ms for the early and 50 ms for the late component). Then, maximal current amplitude was measured in the first 35 ms and in the first 550 ms after the action potential for the two components, respectively. The same measurement was also applied in the backward direction preceding the action potential, where we anticipated no active current. We stated measurable elicited current only if the two sets of amplitudes (measured amplitudes before and after the action potential) significantly differed according to Wilcoxon signed-rank test ($p < 0.05$). At each connection, the average of 5 – 30 traces (11.04 ± 5.05) was used for further analysis.

4.5.2 Excitatory postsynaptic current detection and multiple probability fluctuation analysis

Detection and analysis of EPSCs was performed with NeuroMatic software. Detection threshold was set to 2–4 times the SD of the baseline noise, and onset time limit was set to 2 ms. This defines the maximum delay from the baseline to the deflection threshold. The peak time limit was set to 3 ms. All detected events were inspected by eye. In order to minimize variance originating from temporal fluctuations, we calculated variances using the pairwise method (see Biró, Holderith, and Nusser, 2006 and equation 2 in Scheuss, Schneggenburger, and Neher, 2002). Then to obtain charge (q) and number of functional release sites (N_{FRS}) we plotted the pairwise

variance versus mean and fitted with parabola. The q is estimated as the limiting slope of the parabolic fit and the N_{FRS} as the x intercept of the parabolic fit divided by q. Data points were weighted by the theoretical variance of variance (equations 22-25 in Silver, 2003)

4.5.3 Calcium imaging

We applied a Gaussian filter (standard deviation, σ = 100 ms) to the two-photon calcium imaging traces. When peak amplitude of the event exceeded 3 SD of the baseline fluorescence, we considered it a calcium event. Average frequency and amplitude of the calcium events was measured in a 1 s sliding time window.

4.5.4 Statistics

Data were statistically tested by parametric tests (paired t test or two-sample t test) if they passed the Lilliefors test for normal distribution, and nonparametric tests (Wilcoxon signed-rank test (W SR-test) or Mann–Whitney U test (MW U-test)) were applied in all other cases. Correlations were computed using Pearson's linear correlation coefficient and tested using Student's t-distribution in the astrocyte study, and with Spearman's correlation with testing via t-test in the human study. Error bars and shaded areas show standard deviation.

5 Results

5.1 Interneuron firing-evoked GABAergic volume transmission in astrocytes

5.1.1 Interneuron type-specific signaling to astrocytes

Following reports indicating that certain neocortical interneurons such as neurogliaform cells may be specialized in generating non-synaptic GABAergic responses in nearby cells (Craig and McBain, 2014; Oláh et al., 2009), we performed dual whole-cell patch-clamp recordings from closely spaced (<130 µm) interneuron-astrocyte cell pairs (n = 209), testing the output of n = 164 neurons in layer 1 of the rat somatosensory cortex. All the glial cells recorded had features typical of mature astrocytes (Mishima and Hirase, 2010; Zhou, 2005) showing highly negative membrane potential (–90.2 $\pm$ 3.9 mV) and low input resistance (estimated value: 1.05 $\pm$ 3.94 MΩ). The morphology of the glial cell was recovered in 54 recorded pairs. All 54 recovered glial cells showed characteristic features of an astrocyte (Fig. 5.1 D).

Classification of the recorded interneurons was primarily based on anatomical structure which was recovered in 66 cells. Fifty-three of these were identified as NGFCs and thirteen as non-NGFCs. To extend the classification to interneurons with no anatomical recovery, we developed a cell sorting method. This was based on comparing the electrophysiological parameters of anatomically identified NGFCs

and non-NGFCs by using backward search (Dy and Brodley, 2004; Li, Dong, and Hua, 2008) and scatter separability criteria. This method identified the best electrophysiological feature combination for distinguishing between the two anatomically identified groups of cells (Fig. 5.2). Then, we assigned each recorded cell based on their electrophysiological features to the two anatomically identified groups by Gaussian mixture model (GMM) clustering (Alfó, Nieddu, and Vicari, 2009) ($p < 0.05$). This allowed us to sort the remaining n = 98 neurons with no anatomical recovery into putative neurogliaform (n = 61), putative non-neurogliaform (n = 37) or unidentified groups (n = 28, Fig. 5.2 C).

Responses in astrocytes were studied for single action potentials triggered at 0.011 Hz in the presynaptic interneuron. Analyses revealed that in these conditions none of the non-NGFCs triggered a detectable current in simultaneously recorded astrocyte. In contrast, single action potential in the NGFCs evoked a significant ($p < 0.05$, W SR-test) inward current in 63.1 % of the recorded astrocytes (n = 82 of the 130 pairs tested). Average amplitude of this current was 2.48 ± 1.78 pA (n = 82). These data suggest a cell-type-specific coupling from interneurons to astrocytes (Fig. 5.1).

Further analysis revealed that the NGFC-elicited inward currents consisted of two components, an early component with short (1.6 ms) latency, and a late component with an onset latency about 35 ms from the action potential (Fig. 5.1). The early component had an average amplitude of 0.68 ± 0.45 pA and an average rise time (10–90 %) of 12.9 ± 6.9 ms. Correspondingly, the late component had average amplitude of 1.96 ± 1.89 pA and average rise time of 176.6 ± 87.8 ms (n = 82).

Recordings from interneurons performed in vivo showed sporadic single spikes or brief burst of activity (Gentet et al., 2010); thus, we repeated the experiments above, eliciting a rapid series of action potentials in the interneurons [2–6 action

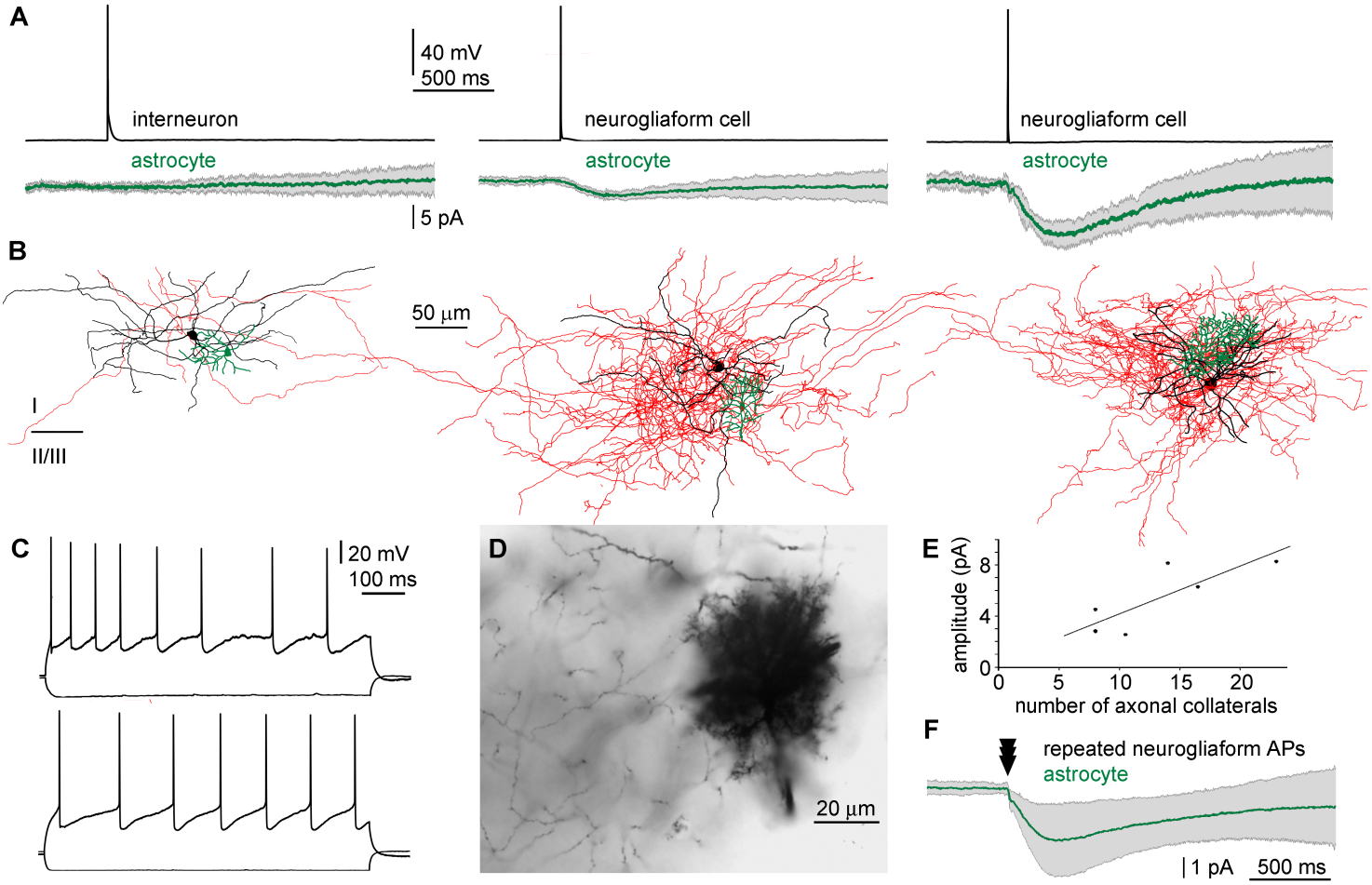

FIGURE 5.1: *Cell-type-specific effect of GABAergic interneurons on astrocytes* **A** Single action potentials in layer 1 non-NGFC interneurons (black, left panel) had no detectable effect on simultaneously recorded astrocytes (green average with gray SD). In contrast, unitary spikes in NGFCs elicited a short-latency, long-lasting inward current in astrocytes (middle and right panel) **B** Anatomical reconstructions of the interneuron–astrocyte pairs shown on A (interneuron somata, black, interneuron axons, red, astrocytic processes, green). Note the axon density around each astrocyte. **C Top**: Firing pattern of the non-NGFC shown in **A** and **B**. **Bottom**: Firing pattern of the NGFC shown in the middle in **A** and **B**. **D** Light microscope micrograph of astrocytic field at the edge of the neurogliaform axon cloud (of the cell in the middle in **B**). **E** Correlations between NGFC-triggered current peak amplitudes in astrocytes and number of axonal collaterals crossing the territory of astrocytes filled with BDA to prevent dye coupling (Pearson's linear correlation, $\rho = 0.82$, $p < 0.05$). **F** Burst of action potentials in NGFCs elicited astrocytic responses with very similar kinetics to the single action potential-triggered responses.

potentials at 44–522, 255 ± 72 Hz (minimum–maximum, mean ± SD)]. Like the single spikes, the burst firing in NGFCs (n = 28) also elicited currents in astrocytes with similar kinetics (Fig. 5.1 F). The current amplitude sublinearly increased with number of action potentials delivered. Interestingly, 24 out of 27 tested non-NGFCs remained completely ineffective (like in the experiments with single spikes). The three non-NGFCs (including one with anatomical recovery) did induce a significant current ($p < 0.05$) in the astrocyte when at least three action potentials (at 262.2 ± 57.4 Hz) were delivered. However, these currents were kinetically different from one another and also from the NGFC-induced currents by visual inspection, rendering statistically reliable analysis impossible.

All interneurons with succesful anatomical recovery and triggering a significant astrocytic current after single action potential exhibited very dense axonal arborization which is typical of NGFCs. By contrast, non-NGFCs, which following single spike had no effect on the astrocytes, displayed relatively sparse axonal arborization (Fig. 5.1). We reconstructed the interacting NGFCs and the spatial boundary of astrocytes filled with biotinylated dextran (n = 6) in three dimensions. When counting the number of neurogliaform axonal collaterals crossing the field of the astrocyte, we found linear correlation with the amplitude of the inward current measured on the astrocyte ($\rho = 0.818$, $p < 0.05$, n = 6, Fig. 5.1 E). The result suggests that the density of the interneuron axon contributes to the effectiveness of connections. Moreover, an inverse correlation between the amplitude of astrocytic inward current and the distance between the tips of the recording electrodes simultaneously placed on the somata of NGFCs and astrocytes was also revealed ($r = -0.306$ $p < 0.05$, n = 82), potentially due to the decrease of axonal density towards the edge of the axonal cloud.

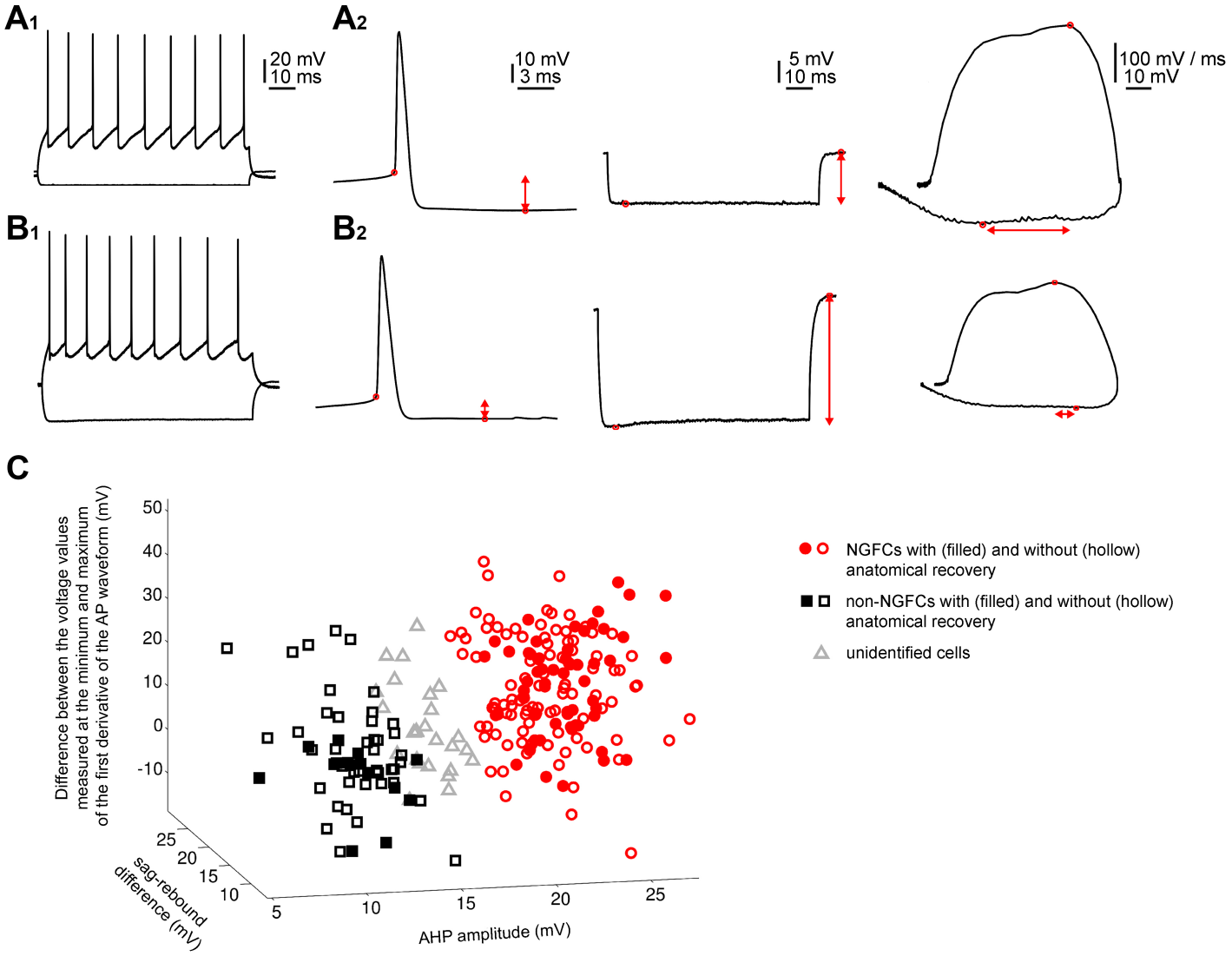

FIGURE 5.2: *Layer I GABAergic interneurons characterized by their electrophysiological features*

A$_1$**, B**$_1$ Firing pattern of a representative NGFC and non-NGFC in layer I (L1). **A**$_2$**, B**$_2$ Three electrophysiological features to best distinguish the two population of interneurons. Red arrows indicate the magnitude of each feature. **Left**: AHP amplitude: Voltage difference (vertical line with arrowheads) measured between the AP threshold and the most negative voltage value following the AP. **Middle**: sag-rebound difference: The voltage difference (vertical arrowed line) between the most hyperpolarized value during the –100 pA current step and the most depolarized value after the current step. **Right**: Difference between the voltage values (horizontal arrowed line) measured at the minimum and maximum of the first derivative of the AP waveform. **C** Classification of all recorded cells based on the three electrophysiological features on A$_2$ and B$_2$. Filled red circles and black squares represent anatomically identified NGFCs and non-NGFCs, respectively. Hollow red circles, black squares and gray triangles represent cells with no anatomical recovery classified by GMM clustering as putative NGFCs, putative non-NGFCs and unidentified cells, respectively.

5.1.2 The astrocytic inward current consists of a direct and an indirect component

The biphasic time course of astrocytic responses to NGFC activation detailed above indicates that potentially complex mechanisms form the basis of these cell-type-specific pathways. Astrocytes are known to participate in potassium clearance from the extracellular space (Amzica, Massimini, and Manfridi, 2002; Kofuji and Newman, 2004). Therefore, we bath applied $BaCl_2$, a concentration-dependent blocker of GIRK and KIR channels (Hibino et al., 2010) in search for potential K^+ currents. These experiments revealed an early, barium-insensitive and a late, barium-sensitive component of the astrocytic inward current induced by single action potentials in NGFCs. When applied at low concentrations (5 µM–10 µM), $BaCl_2$ significantly reduced the late component probably acting mainly on GIRK channels (from 4.35 ± 1.71 pA to 1.59 ± 0.82 pA, $p < 0.01$, $n = 5$, Fig. 5.3) without affecting the early component. In addition, high $BaCl_2$ concentration (100 µM) completely abolished the late component (from 1.80 ± 1.32 pA to 0.08 ± 0.18 pA, $p < 0.01$, $n = 7$). Interestingly, this also increased the early component (from 1.17 ± 0.57 pA to 2.71 ± 1.26 pA, $p < 0.01$, $n = 7$). Although reason for this counter-intuitive result is not fully clear, one explanation is broadening of the NGFC action potentials (from 0.77 ± 0.12 ms to 0.85 ± 0.13 ms full width at half maximum amplitude, $p < 0.05$, $n = 7$) which is known to increase the presynaptic neurotransmitter release. This suggests that the early component is generated by the GABA released. Furthermore, a GABA-induced current could also be increased in these conditions simply by improved space clamp properties of the voltage clamp recording. In other words, astrocytic currents measured in the voltage clamp mode can theoretically be increased if the high levels of barium substantially block the astrocyte's KIR channels and reduce the astrocyte input resistance (Hibino et al., 2010; Ma et al., 2014; Williams and Mitchell, 2008).

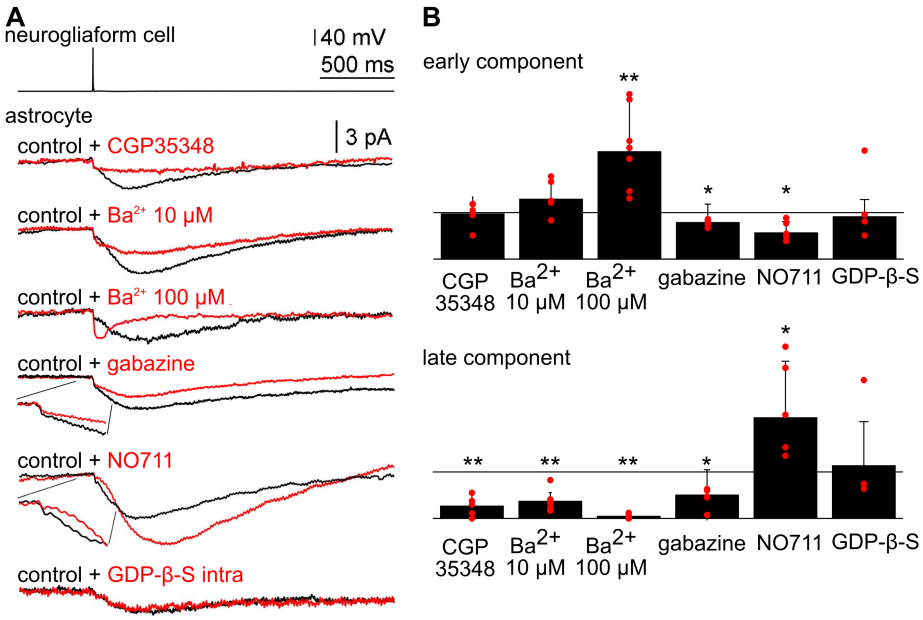

FIGURE 5.3: *Neurogliaform cell triggered, unitary GABAergic currents in astrocytes are mediated by $GABA_A$ receptors, GABA transporters, and $GABA_B$ receptors.*

A NGFC single spike-triggered astrocytic current is sensitive to extracellularly applied $GABA_B$ receptor antagonist (CGP35348), a potassium channel blocker (Ba^{2+}), a $GABA_A$ receptor antagonist (gabazine), a GABA transporter blocker (NO711), but not to intracellularly applied G-protein-coupled receptor antagonist (GDP-β-sulfate, GDPBS). **B** Summary of the drug effect data including all astrocytes studied. **Top**: Early component of the astrocytic current. **Bottom**: Late component of the astrocytic currents. Data are normalized in individual experiments by amplitude in baseline (horizontal line, 100 %) measured before drug application. Peak amplitude of the early and the late component was measured 0 ms–35 ms and 35 ms–550 ms following the NGFC action potential, respectively.Traces are the averaged from all recordings. Asterisks indicate significant difference (*$p < 0.05$; **$p < 0.01$)

Following pioneering reports showing that $GABA_A$ receptors depolarize astrocytes (Kettenmann, Backus, and Schachner, 1984) and given that NGFCs release GABA (Tamás et al., 2003), we tested whether $GABA_A$ receptor activation contributes to the single-cell-evoked astrocytic currents. Bath application of gabazine (5 µM), a specific $GABA_A$ receptor blocker, significantly reduced both the early potassium-independent and the late potassium-dependent inward current (from 1.28 ± 0.62 pA to 1.01 ± 0.51 pA, $p < 0.05$, $n = 5$ for the early component and from 1.76 ± 1.52 pA to 0.88 ± 0.61 pA, $p < 0.05$, $n = 5$ for the late component, Fig. 5.3). The effect of $GABA_A$ receptor blockade shows that both the early and the late component are dependent on $GABA_A$ receptor activation. Yet, the result does not show whether the $GABA_AR$ effect is direct ($GABA_A$ receptors activated on the recorded astrocyte) or indirect ($GABA_A$ receptors not activated in the astrocyte but in nearby cells and their activity generates secondary effect seen as a current in the astrocyte). One possible explanation is that there is a direct $GABA_A$ receptor activation in the early component and the subsequent increase in extracellular K^+ ions due to the neuronal potassium-dependent chloride extrusion (Kaila et al., 1997; Viitanen et al., 2010) in the late component. These results suggest that GABA released from single neurogliaform axons non-synaptically acts on astrocytic $GABA_A$ receptors, inducing chloride and probably bicarbonate ion efflux and, furthermore, confirm the contribution of potassium-dependent Cl^- transport to neurogliaform-to-astrocyte signaling.

In addition to $GABA_A$ receptors, astrocytes express GABA transporters which uptake the neurotransmitter from extracellular space. The transporter is driven by an inward Na^+ current in astrocyte (Doengi et al., 2009; Eulenburg and Gomeza, 2010). Bath application of GABA uptake inhibitor NO711 (100 µM) alone reduced the early component of the astrocytic current (from 1.21 ± 0.51 pA to 0.68 ± 0.29 pA,

$p < 0.05$, n = 6, Fig. 5.3). The result suggest that GABA released from a neurogliaform cell by single action potential acts directly on the astrocyte by activation of electrogenic GABA uptake transporter, which contributes to the early inward current. On the contrary, NO711 significantly increased the amplitude of the astrocytic late component (from 3.27 ± 2.18 pA to 7.08 ± 3.98 pA, $p < 0.05$, n = 6) and prolonged the rise time (10–90 %) (from 203 ± 16 ms to 310 ± 49 ms, $p < 0.01$). Thus, the opposite effect of NO711 on the late component indicates the increased GABA effect on the astrocyte which depolarizes it by $GABA_A$ receptor activation and extracellular potassium accumulation.

The astrocytic late component was also sensitive to the selective $GABA_B$ receptor antagonist CGP35348 (40 µM), which reduced the late current (from 1.77 ± 0.99 pA to 0.45 ± 0.42 pA, $p < 0.01$, n = 6, Fig. 5.3) reminiscent of the $BaCl_2$ application experiment that blocked potassium channels. Thus, the late component appears to be mediated by chloride extrusion mechanisms and $GABA_B$ receptors coupled to K^+ channels, and, as such, it is amplified by GABA transporter blockade. However, given the high-resolution immunohistochemical and *in situ* hybridization results of independent reports, which failed to detect $GABA_B$ receptors on mature astrocytes (Fritschy et al., 2004; Kaupmann et al., 1997; López-Bendito et al., 2004; Luján and Shigemoto, 2006; Martin et al., 2004), the $GABA_B$ receptors responsible for the recorded current might not reside on the astrocytes. To test this hypothesis, we aimed to block $GABA_B$ receptors in the astrocytes intracellularly, using G-protein blocker GDP-β-S (1 mM) in intracellular solution. Indeed, this resulted in no significant changes in the astrocytic current (Fig. 5.3). For control, we tested the efficacy of the drug in neurogliaform-to-pyramidal cell pairs where single NGFC action potential evokes $GABA_B$ receptor-mediated IPSP. We confirmed the intracellular GDP-β-S containing solution was viable since it abolished the $GABA_B$ component of synaptic

IPSPs in all studied pyramidal cells under the same conditions (n = 3). These results suggest that the late astrocytic inward current is generated for the most part by activation of neuronal $GABA_B$ receptors, which leads to transient accumulation of potassium ions in the interstitial space though $GABA_B$ receptor activated potassium efflux from neurons. Transiently elevated extracellular potassium concentration directly depolarizes the astrocyte throught inwardly rectifying potassium channels following Nerstian equation (Hille, 1992).

5.1.3 Physiological GABA release fails to elicit detectable calcium transients in surrounding astrocytes

Astrocytes exhibit intense local changes in intracellular Ca^{2+} activity (Di Castro et al., 2011; Grosche et al., 1999; Volterra, Liaudet, and Savtchouk, 2014), the dynamics of which were suggested to be modulated by GABAergic signaling through various mechanisms. The activation of $GABA_A$ receptors has been reported to elicit Ca^{2+} signals in astrocytes through membrane depolarization and subsequent voltage-dependent Ca^{2+} channel recruitment (Meier, Kafitz, and Rose, 2008). Yet, previous experiments on the GABA effect are based on externally applied ligand and effectiveness of endogenously released GABA in the astroglial Ca^{2+} dynamics is yet to be established (Vélez-Fort, Audinat, and Angulo, 2012).

Increased Ca^{2+} dynamics following astrocytic GABA receptor activation has repeatedly been observed (Kang et al., 1998; Nilsson et al., 1993; Serrano et al., 2006). However, $GABA_B$ receptor-mediated Ca^{2+} events can only be detected in cultured astrocytes, which are known to be different from mature cells (Cahoy et al., 2008). This conclusion is in line with observations that $GABA_B$ receptor-mediated astrocytic Ca^{2+} signals also occur in young animals (Meier, Kafitz, and Rose, 2008) consistent with transient expression of $GABA_B$ receptors in astrocytes (Fritschy et al.,

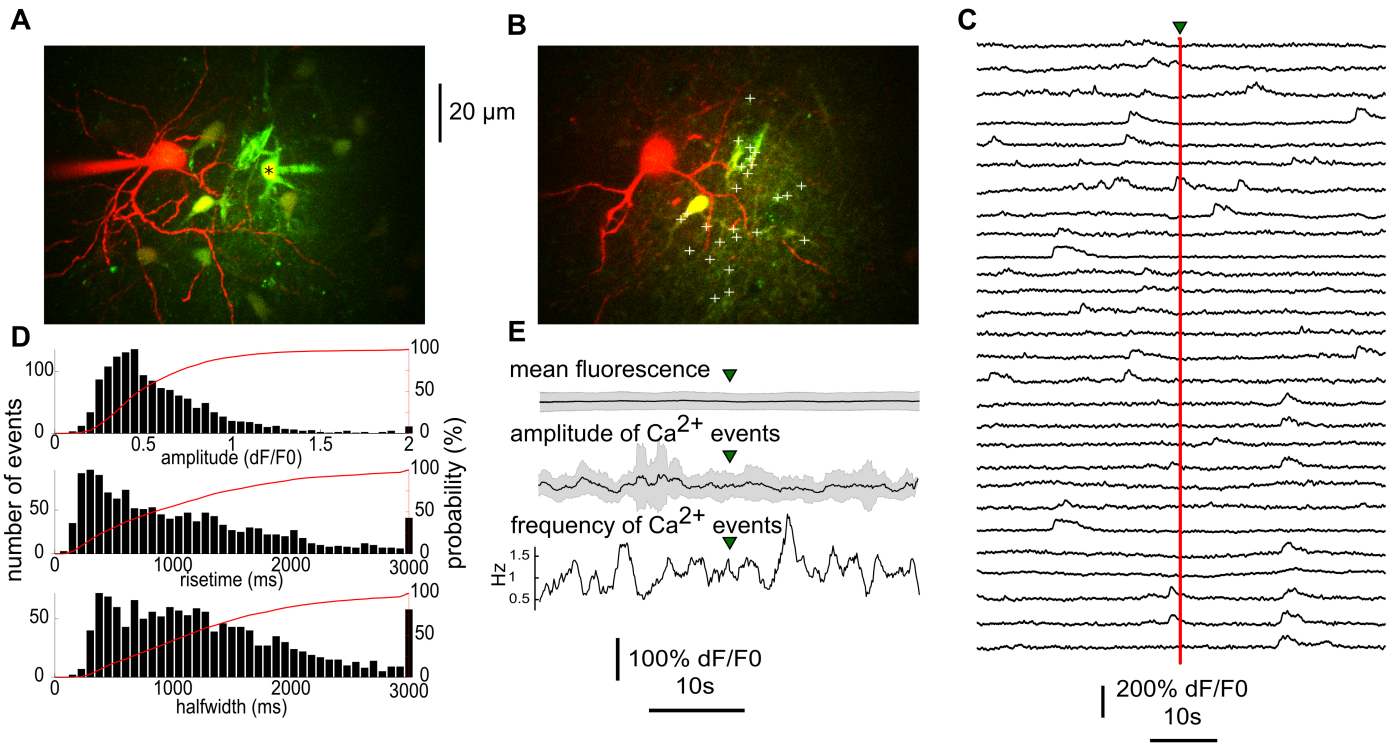

FIGURE 5.4: *Dynamics of calcium transients in astrocytes following single spikes in nearby NGFC.*

A Two photon Z-stack image showing a simultaneously whole-cell recorded NGFC (red) and an astrocyte (green). Several neighboring astrocytes are dye coupled to the recorded astrocyte (asterix) possibly through gap junctions. **B** A representative image in single optical plane showing regions (white crosses) to measure calcium activity level in astrocyte processes. **C** Examples of Ca^{2+} activity in the marked regions shown in B. Arrowhead and red line indicates timing of NGFC spike. **D** Amplitude (dF/F0), rise time, and half amplitude width of all calcium transients detected in astrocytes studied (n=5). Bar histogram scaling on left. The same data are plotted in a cumulative histogram (red line, scaling on right). **E** Mean fluorescence intensity, amplitude, and frequency of astrocytic calcium transients prior to and following single action potential in NGFCs (timing indicated by arrowhead). Data are averaged in 1 s long sliding time window (black = average, gray = SD of all recordings).

2004; López-Bendito et al., 2004; Luján and Shigemoto, 2006).

To study the Ca^{2+} signals in both astrocyte somata and processes (Volterra, Liaudet, and Savtchouk, 2014), we intracellularly filled (Di Castro et al., 2011) individual astrocytes in close vicinity (<70 µm) of identified NGFCs with the calcium indicator OGB-1 (120 µM) and a calcium-insensitive structure dye Alexa Fluor 594 (40 µM, Fig. 5.4 A,B). Next, we randomly selected 100–300 regions of interest (ROIs) on the soma and processes of the intracellularly filled astrocyte. In addition, this method allowed us to place ROIs on neighboring astrocytes which were dye coupled through gap junctions. We readily detected spontaneous Ca^{2+} events of variable amplitude and duration (Fig. 5.4 D). However, we did not detect an increase in their amplitude or frequency following single action potentials in the nearby NGFCs (Fig. 5.4 C,E). The result was very interesting, because previous reports had shown astrocytic calcium modulation by exogenously applied GABA or GABAergic interneuron activation (Kang et al., 1998; Meier, Kafitz, and Rose, 2008; Nilsson et al., 1993; Serrano et al., 2006). Our results suggest that magnitude of physiologically-evoked GABA-mediated inward current in astrocytes is not sufficient to depolarize the cells to recruit voltage-gated Ca^{2+} channels, and furthermore, it also indicates the absence of $GABA_B$ receptor activation-dependent Ca^{2+} signaling on mature astrocytes.

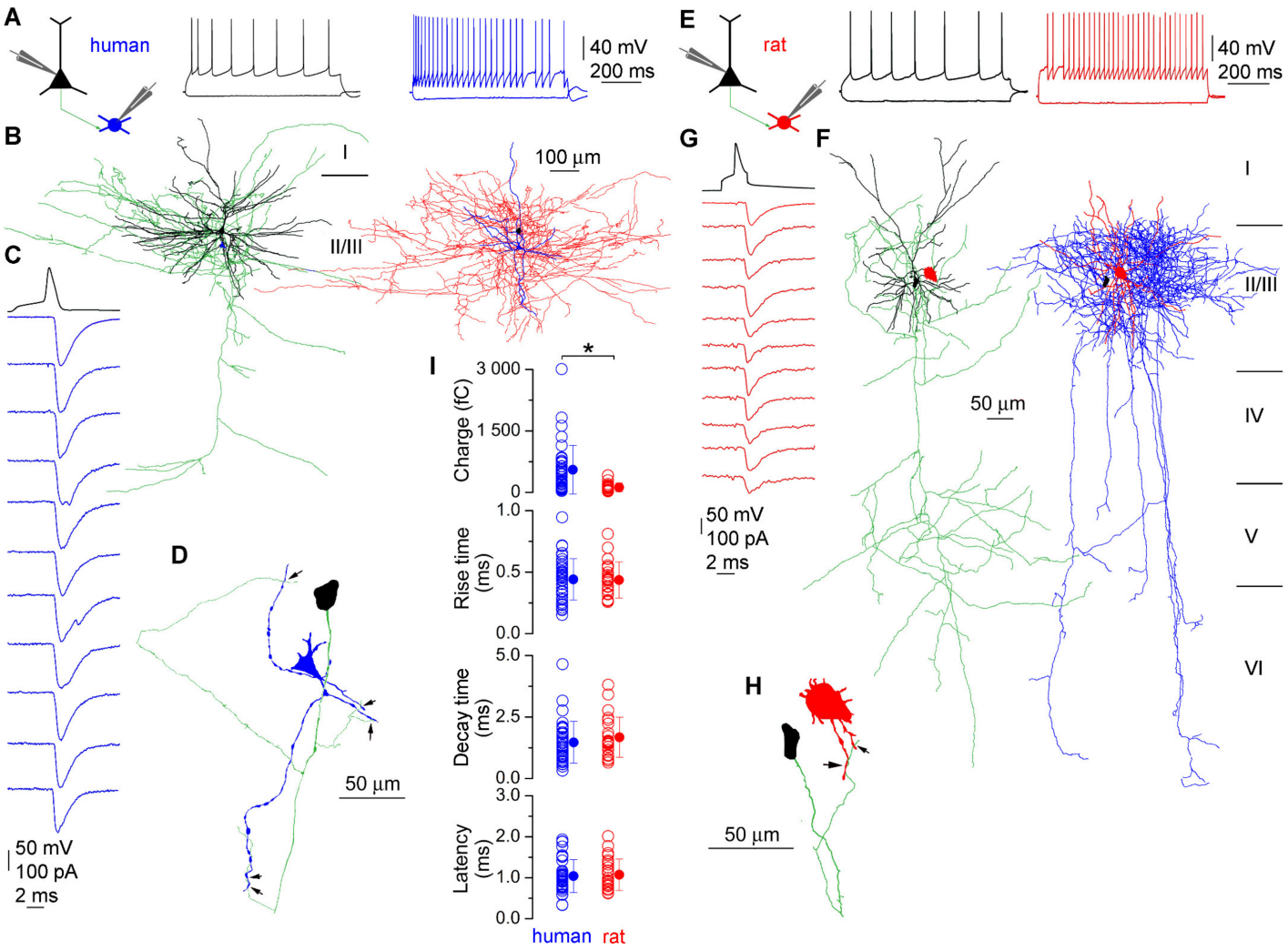

FIGURE 5.5: *Monosynaptic excitatory connections from pyramidal cells to interneurons in the human and rat cerebral cortex.*

A Firing pattern of a presynaptic pyramidal cell (black) and a postsynaptic basket cell (blue) simultaneously recorded in layer 2-3 in an acute slice of the human neocortex. **B** Light microscopy reconstruction of the recorded pyramidal cell (**left**, soma and dendrites in black, axons in green) and basket cell (**right**, soma and dendrites in blue, axons in red). Scale bars apply to both cells. Reconstructions of the cells are separated for clarity with relative positions of the somata (pyramidal cell in black, basket cell in blue) indicated on both panels. Roman numbers represent neocortical layers from I to VI. **C** Single presynaptic action potentials of the pyramidal cell (sample black trace) elicited unitary EPSCs (blue traces) in the basket cell (held at –70 mV) Top blue trace shows their average. **D** Route of the presynaptic axon (green) from the PC soma (black) making putative synaptic contacts (arrows) in juxtaposition to the basket cell dendrites (blue). **E–H** A rat pyramidal cell to basket cell connection presented in similar panels as A–D. **I** Evoked unitary EPSCs in the human and rat have similar latency, rise and decay time. However, the human EPSC charge is substantially larger.

5.2 Species specific features of supragranular pyramidal cell to interneuron synapses

5.2.1 Quantal parameters of pyramidal cell to fast-spiking interneuron EPSCs in the human and rat cerebral cortex

We compared the functional properties of synaptic connections made by pyramidal cells onto fast-spiking interneurons in the layer 2/3 of human (n = 39) and rat (n = 26) neocortex (Fig. 5.5). Acute human brain slices were prepared from small blocks of non-pathological samples of frontal, temporal and parietal neocortical tissue resected in surgeries from female (n = 15, aged 53 ± 13 years) and male (n = 11, aged 43 ± 24 years) patients (Komlósi et al., 2012; Molnár et al., 2008). Correspondingly, rat brain slices were prepared from somatosensory cortex of juvenile (p18–28, n = 9) and prefrontal cortex of adult (p53–65, n = 8) male rats using standard acute slice preparation procedures (Oláh et al., 2007). Both presynaptic pyramidal cells and postsynaptic interneurons were recorded in whole-cell configuration using biocytin-containing intracellular solutions, allowing *post hoc* identification of the recorded cell types and the number of synaptic contacts between them. Neurons were chosen based on their typical membrane and firing properties. Postsynaptic interneurons were identified as either axo-axonic (AACs, human: n = 6) or basket (BCs, human: n = 18; rat: n = 8) cells based on their characteristic axonal cartridges or axonal branches forming perisomatic baskets, respectively (Klausberger and Somogyi, 2008).

Excitatory postsynaptic currents, recorded from the interneurons in response to single presynaptic pyramidal cell action potentials showed a wide range of amplitudes in both species (human: 9.0 pA–1477.1 pA; rat: 7.7 pA–236.3 pA), but with a

significantly larger mean amplitude in human interneurons (human: 258.8 ± 272.8 pA; rat: 75.8 ± 58.7 pA; $p < 0.001$, MW U-test). Otherwise the evoked unitary EPSCs in the human and the rat had similar features: Latency (human: 1.04 ± 0.40 ms, n = 37; rat: 1.10 ± 0.38 ms, n = 25; p = 0.79, MW U-test), rise time (10–90 %, human: 0.44 ± 0.16 ms, n = 39; rat: 0.43 ± 0.14 ms ms; n = 26; p = 0.95, MW U-test) and decay time (37 %, human: 1.46 ± 0.83 ms, n = 38; rat: 1.7 ± 0.8 ms, n = 26; P = 0.18, MW U-test). In addition, the larger amplitude with similar decay resulted in a significantly larger EPSC charge in human (human: 553.6 ± 593.3 fC, n = 38; rat: 123.1 ± 107.6 fC, n = 26; $p < 0.001$, MW U-test, Fig. 5.5).

The synaptic current in a given synaptic connection is dependent on the quantal parameters, which are the quantal size (q), number of functional release sites (N_{FRS}) and release probability (Pr) (Katz, 1969). To determine quantal parameters of synaptic connections, we performed multiple probability fluctuation analysis (MPFA, (Clements and Silver, 2000; Silver, 2003); human: n = 10, rat: n = 12, Fig. 5.6). Different release probability conditions were imposed by altering Ca^{2+} and Mg^{2+} ion concentrations in the extracellular solution during recordings (Silver, 2003) and measured the means and variances of EPSC charge. These recordings were performed in the presence of an NMDA and a cannabinoid receptor antagonist (20 µM D-AP-5 and 10 µM AM251, respectively) to prevent NMDA channel openings, which might reduce variances and induce long-term plasticity (Saviane and Silver, 2007; Silver, 2003) and to exclude undesirable retrograde short- or long-term modification of glutamatergic transmission (Lee, Földy, and Soltesz, 2010; Péterfi et al., 2012) during MPFA. In addition, low affinity competitive non-NMDA receptor antagonist γDGG (0.5 mM) was included to prevent AMPA receptor saturation (Sakaba, Schneggenburger, and Neher, 2002; Scheuss, Schneggenburger, and Neher, 2002; Wadiche and Jahr, 2001). To avoid rundown of EPSCs during long-lasting

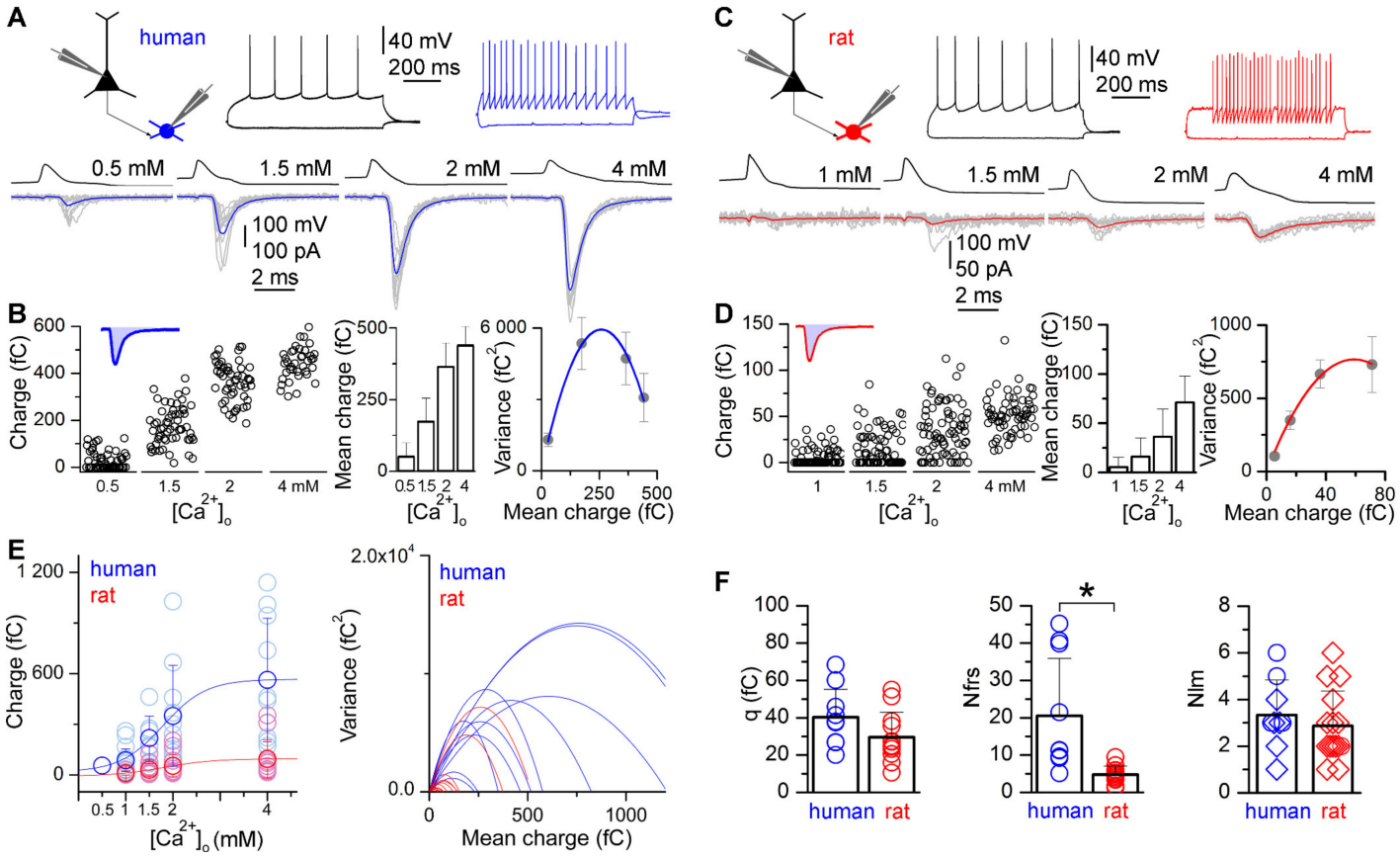

FIGURE 5.6: *Higher number of functional release sites in the human excitatory synapses is revealed by multiple probability fluctuation analysis (MPFA).*

A Firing pattern of a human pyramidal cell (black) monosynaptically connected to a postsynaptic basket cell (blue). **Bottom**: Pyramidal cell action potential-evoked EPSCs in the basket cell recorded in different extracellular calcium concentrations ($[Ca^{2+}]_o$ in mM) 0.5, 1.5, 2 and 4 (grey = 10 consecutive traces, blue = averages). **B Left**: Charge transferred by the evoked unitary EPSCs in different $[Ca^{2+}]_o$. Inset EPSC trace with shaded blue area illustrates the charge of an EPSC. **Middle**: Mean ± SD of the EPSC charge in the same experiment. **Right**: Parabolic fit to the variance versus mean of the EPSC charge recorded in different $[Ca^{2+}]_o$. The function allows to estimate the quantal size (q = 45.9 fC, as the limiting slope of the parabolic fit) and the number of functional release sites (N_{FRS} = 11.3, as the x intercept of the parabolic fit divided by q). **C–D** A similar experiment illustrated in a rat pyramidal cell (black) to basket cell (red) connection (N_{FRS} = 4.9; q = 25.0 fC). **E Left**: Dependence of the EPSC charge in human (blue) and rat (red) on the $[Ca^{2+}]_o$ **Right**: Parabolic fits to the variance versus mean plots in human (blue) and rat (red). **F** Multiple probability fluctuation analysis of human and rat unitary EPSCs does not show significant difference in quantal size (human: 40.2 ± 14.9 fC, n = 10; rat: 29.6 ± 13.3 fC, n = 12; p = 0.11, MW U-test). Yet it indicates that the number of functional release sites is substantially larger in the human compared to rat (human: 20.5 ± 15.4, n = 10; rat: 4.7 ± 2.3, n = 12; $p < 0.001$, MW U-test). However, the number of contact sites detected with light microscopy (Nlm) between presynaptic axons and postsynaptic dendrites is similar in human and rat (right, human: 3.3 ± 1.5, n = 9; rat: 2.9 ± 1.5, n = 15, p = 0.36, MW U-test). The Nlm plot indcludes data from reconstructions with and without MPFA (shown by circles and diamonds, respectively).

recordings, 10 mM L-glutamate was added to the internal solution of the presynaptic cell (Biró, Holderith, and Nusser, 2005; Ishikawa, Sahara, and Takahashi, 2002). As expected, the amplitudes of human and rat unitary EPSCs were effectively modulated by altering extracellular Ca^{2+} and Mg^{2+} ion concentrations, consistent with changes in the probability of release (Pr) of a vesicle at a functional release site. EPSC failure rates were significantly lower in human neurons ($p < 0.012$, MW U-test) in each condition compared to rats (1 mM $[Ca^{2+}]_o$: 15.8 ± 18.7 % vs. 62.8 ± 34.2 %, 1.5 mM $[Ca^{2+}]_o$: 2.0 ± 4.0 % vs. 39.1 ± 24.7 %, 2 mM $[Ca^{2+}]_o$: 0 vs. 26.6 ± 21.7 %, 4 mM $[Ca^{2+}]_o$: 0 vs. 8.4 ± 10.2 %). The different failure rates indicate either release probability for individual vesicles or a different number of functional release sites (N_{FRS}). This approach resulted in a large, 10- and 5.5-fold increase in the mean charge transferred by human and rat unitary EPSCs, respectively from the lowest to the highest $[Ca^{2+}]_o$, which is a prerequisite for reliable determination of the quantal parameters (Silver, 2003). By fitting the mean vs. variance relationship with a parabola, we obtained an estimate of quantal size, Pr and N_{FRS} for each cell pair. Statistical comparisons of data from all cells revealed no significant difference in quantal size ($p = 0.11$, MW U-test). Yet, we found significant difference in the Pr (at 1.5 mM $[Ca^{2+}]_o$: human: 0.33 ± 0.10, range: 0.18–0.48, $n = 7$; rat: 0.17 ± 0.13, range: 0.05–0.53, $n = 12$; $p < 0.01$, MW U-test). Furthermore, our analysis revealed a 4.4-times larger N_{FRS} in human connections (20.5 ± 15.4, range 5.1–45.2) compared to rats (4.7 ± 2.2, range 1.3–9.5; $p < 0.001$, MW U-test, Fig. 5.5 F).

5.2.2 Structural features of pyramidal cell synapses to fast-spiking interneurons in the human and rat cerebral cortex

A potential explanation for the differences in EPSC amplitudes and N_{FRS} between the human and rat is simply a larger number of synaptic contacts connecting the PC

axons to the postsynaptic IN dendrites in the human cortex. To assess the number of putative synaptic contacts, team members without access to the N_{FRS} searched for close appositions of presynaptic axon terminals and postsynaptic dendrites under light microscopy (LM). The presynaptic axon from the parent pyramidal cell soma to the target interneuron dendrites were reconstructed in nine human (n = 2 PC to AAC and n = 7 PC to BC pairs) and fifteen rat (n = 15 PC to BC pairs) pairs that partially overlapped with MPFA analyzed cell pairs. Yet, we found no difference in the number of LM detected synaptic contacts (N_{LM}) between the human (3.3 $\pm$ 1.5; range: 1–6) and the rat (2.9 $\pm$ 1.5, range: 1–6) (p = 0.35, MW U-test, Fig. 5.5 F). Consequently, dividing the mean N_{FRS} with the mean N_{LM} indicated that each presynaptic bouton contains on average 6.2 and 1.6 functional release sites in human and rat, respectively. This ratio was also larger for human connections when calculated from those pairs for which both MPFA and LM reconstructions could be performed (human: N_{FRS}/N_{LM} = 5.7 $\pm$ 5.1, range 1.6–13.3, n = 4; rat: N_{FRS}/N_{LM} = 2.6, n = 1). These results demonstrate that differences in the number of synaptic junctions between PCs and fast-spiking interneurons is not responsible for the observed 4.4-fold larger N_{FRS}, therefore each presynaptic PC axon terminal must contain a larger N_{FRS} in human. Finally we looked for potential ultrastructural correlates of the above described differences in the N_{FRS} in individual axon terminals. We performed three-dimensional reconstructions of presynaptic axon terminals from 20 nm thick serial EM sections. Biocytin-filled, *post hoc* recovered human (n = 3) and rat (n = 3) INs were chosen and axon terminals that established asymmetrical synaptic contacts on selected dendrites were fully reconstructed (Fig. 5.7). First we compared the size of presynaptic active zones (AZs) and found that both human and rat active zones have variable sizes (human: 0.02–0.26 mm^2; rat: 0.02–0.08 mm^2), but the human AZs were on average twice as large. Each bouton contained only a single AZ in

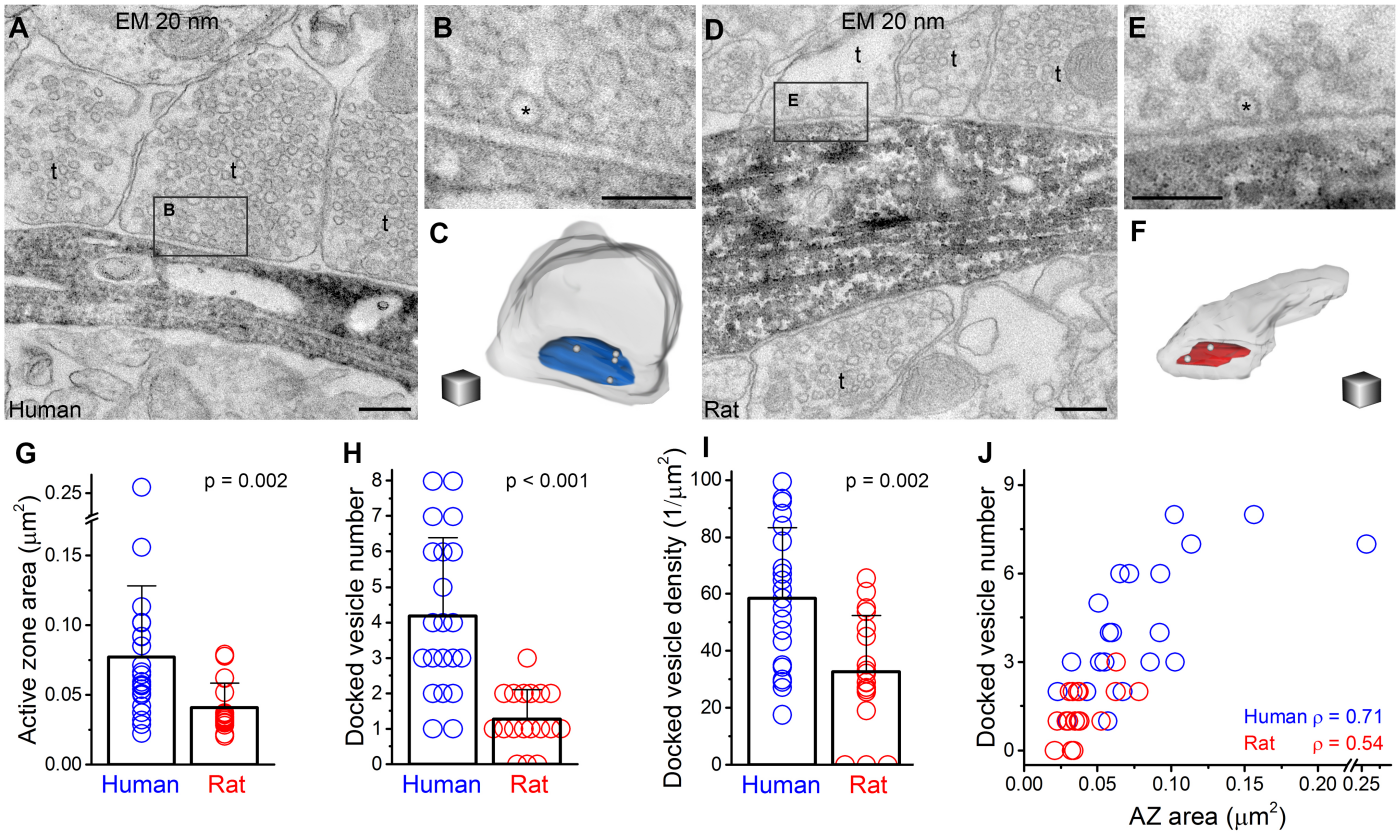

FIGURE 5.7: *Active zones (AZs) of excitatory synapses are twice as large and harbor four times as many docked vesicles in humans as in rats.*

A,D Electron microscopic images of 20 nm thick sections show axon terminals forming asymmetrical synapses on a human (A) and a rat (D) fast spiking interneuron dendrite in layer 2-3. The intracellularly biocytin-filled interneuron is visualized with peroxidase reaction generating the dark precipitate. **B, E** Higher magnification view of the boxed areas in A and H, showing docked vesicles (*) in the AZs. **C, F** 3D reconstructions of the terminals shown in B and D. The human terminal (C, grey semitransparent contour) contains an AZ (blue) of 0.09 μm^2 with four docked vesicles (white spheres). On the contrary, the rat AZ (red in F) is 0.04 μm^2 and has two docked vesicles. **G** The area of AZs, determined from 3D reconstructions from 20 nm thick serial sections, is twice as large in the human (0.077 $\pm$ 0.051 μm^2, n = 22, from three separate human samples; rat: 0.041 $\pm$ 0.017 μm^2, n = 19 from three animals; $p < 0.01$, MW U-test). **H** Number of the docked vesicles, identified in fully reconstructed AZs from 20 nm serial sections, is four times larger in the human (human: 4.2 $\pm$ 2.2, n = 21) compared to the rat (1.3 $\pm$ 0.8, n = 18) ($p < 0.001$, MW U-test). **I** The density of docked vesicles, measured in 20 nm reconstructions (human: 58.5 $\pm$ 24.6 μm^{-2}, n = 21, rat: 32.5 $\pm$ 19.9 μm^{-2}, n = 18, $p < 0.001$, unpaired t-test), is significantly different between the two species. **J** The number of the docked vesicles shows a positive correlation with the AZ area (human: $\rho = 0.71$, $p < 0.01$; rat: $\rho = 0.54$, $p < 0.05$, Spearman correlation tested via t-test). Scale bars: A, D: 200 nm, B, E: 100 nm, C, F: 200 nm

both species. When we counted docked vesicles in these AZs using the 20 nm thin serial section approach we found a significantly larger number in human (4.2 ± 2.2 / AZ) compared to rats (1.3 ± 0.8 / AZ; $p < 0.001$, MW U-test), resulting in a twice as large docked vesicle density in human. The large variability in the AZ area and number of docked vesicle prompted us to investigate their relationship and found a positive correlation between these parameters in both species (human: $\rho = 0.71$, $p < 0.01$; rat: $\rho = 0.54$, $p < 0.05$, Spearman correlation tested via t-test).

6 Discussion

6.1 Physiological GABAergic volume transmission from interneurons to astrocytes in the rodent cerebral cortex

Non-synaptic or volume transmission acts ubiquitously on all –neuronal and non-neuronal– target elements expressing receptors for the released transmitter (Vizi and Kiss, 1998). Neurogliaform cells were suggested to operate by flooding the axonal arborization with GABA, resulting in a single-cell-driven volume transmission (Oláh et al., 2009). The results presented here extend this concept and identify a cell-type-specific route for interneuron to astrocyte signaling in addition to the conventional GABAergic output toward neurons. Neurogliaform cell to astrocyte communication has several GABAergic elements. The early component has a contribution of currents mediated by $GABA_A$ receptors and GABA transporters, and its short latency indicates a direct communication pathway from NGFCs to astrocytes. We cannot rule out the possibility of electrotonic coupling between NGFCs and astrocytes based on these data; however, the latency of 1.6 ms strongly suggests that there is no gap junctional current in the early component (Simon et al., 2005). The second, indirect GABAergic pathway involves the activity of chloride transporters and $GABA_B$ receptors presumably located on neuronal elements of the circuit, and

the resulting extracellular accumulation of K^+ is taken up by astrocytes as the late component. The net result of this cascade of events is the transport of K^+ through the extracellular space and a transient rise in Cl^- and/or bicarbonate in the extracellular space. Both of these factors contribute to the suppression of neuronal excitability by membrane hyperpolarization and by maintaining the driving force of GABAergic synapses, respectively.

Importantly, these mechanisms are activated while NGFCs act on $GABA_A$ and $GABA_B$ receptors on dendritic compartments and $GABA_B$ receptors on presynaptic terminals of neighboring neurons (Capogna, 2011; Chittajallu, Pelkey, and McBain, 2013; Oláh et al., 2009). These simultaneous and densely packed inhibitory currents on the neuronal processes are counteracted by the currents on the surrounding astrocytes thus are stabilized and made more effective. Furthermore, astrocytic GABA transporter activation might lead to the downregulation of local excitatory collaterals (Boddum et al., 2016). Interestingly, certain operational states of the microcircuit might require several elements of this effective simultaneous inhibition. For example, UP to DOWN state transition in the cerebellar cortex is linked to the increase in the extracellular K^+ concentration (Wang et al., 2012), to local interneuronal activation (Oldfield, Marty, and Stell, 2010), and to $GABA_B$ receptor activation (Craig et al., 2013; Mann, Kohl, and Paulsen, 2009). We propose that neurogliaform-to-astrocyte interactions contribute to inhibitory scaling in the neocortex through multiple non-synaptic mechanisms.

Astrocytes were repeatedly shown to actively participate in neurotransmission with propagating intracellular calcium waves and gliotransmitter release. However, our results demonstrate a passive role of astrocytes in a unitary GABAegic communication pathway. This discrepancy is not new to this field and has generated a heated debate recently (Fiacco and McCarthy, 2018; Savtchouk and Volterra,

2018). The source of this controversy might be the different experimental procedures used. Our experiments were performed in brain slices prepared from young adult rats (p25–46, p37.4 $\pm$ 4.5) where the electrophysiological, anatomical and molecular properties of astrocytes are considered mature (Bushong, Martone, and Ellisman, 2004; Bushong et al., 2002; Cahoy et al., 2008; Freeman, 2010; Meier, Kafitz, and Rose, 2008; Mishima and Hirase, 2010; Ogata and Kosaka, 2002; Sun et al., 2013; Zhou, 2005). In contrast, previous studies showing astrocytic calcium signalling due to $GABA_B$ receptor activation (Covelo and Araque, 2018; Kang et al., 1998; Mariotti et al., 2018; Meier, Kafitz, and Rose, 2008) or gliotransmission (Fiacco and McCarthy, 2018; Sloan and Barres, 2014), were shown mainly in cell cultures or in slice preparations from young rodents (p12-p25), in the timeframe where synaptogenesis takes place (Freeman, 2010). Interestingly, even the most recent articles supporting $GABA_B$ receptor presence and signalling in astrocytes of the adult cortex utilize young rodents for their key experiments (Covelo and Araque, 2018; Mariotti et al., 2018), probably due to technical limitations. We hypothesize that astrocytes are involved in $GABA_B$ receptor dependent calcium signaling only in young rodents before astrocytes gain their mature functions.

6.2 Species specific differences in pyramidal cell synapses to GABAergic interneurons

Paired recordings, MPFA and post hoc anatomical reconstructions revealed that presynaptic AZs contain on average 6 functional release sites in human, but only 1.6 in rats. High resolution EM analysis identified corresponding species-specific differences in the AZ area and the number of docked vesicles. Our data allowed us to provide the first estimate of the size of Katz's functional release site (Castillo

and Katz, 1954) of cortical synapses; approximately 0.012 µm^2 AZ membrane area in human and 0.025 µm^2 in rats. Thus, the space that harbors a functional release site or a docking site seems to be substantially smaller in human AZs. This raises an interesting question: why the molecular machinery necessary for the assembly of a functional release site needs less space in human? Answering this question requires quantitative proteomic analysis of these AZs at nanometer resolutions. Furthermore, it will be also interesting to see whether this species-specific difference is valid for all central synapses or it is a unique feature of the cortical microcircuit.

Our data demonstrating that an AZ in rat PC axons contains on average a single functional release site is consistent with the 'one site-one vesicle' hypothesis (Korn et al., 1982) and with data previously published for rodent cortical and hippocampal excitatory synapses (Biró, Holderith, and Nusser, 2005; Gulyás et al., 1993; Silver, 2003). In contrast, the same type of axon terminals in human contain on average 6 functional release sites, demonstrating that here multivesicular release (MVR; Rudolph et al., 2015) is the main mode of operation. However, it is important to note that our data clearly demonstrate large variability in the AZ area in both species and that the number of docked vesicles and docking sites correlates with the AZ area. Thus, MVR is not a human-specific feature of cortical synapses, but it is expected to occur at large AZs of this connection in rats, as it has been shown to take place in many other rat glutamatergic synapses (Rudolph et al., 2015). Comparison of the N_{FRS} and the number of docked vesicles allowed the calculation of the average docking site occupancy that is 0.8 in rats and $\approx$ 0.7 in human synapses, similar to that calculated for the Calyx of Held (Neher, 2010), and somewhat higher than that found in cerebellar interneuron synapses (Pulido et al., 2015). Similarly large docking site occupancy and vesicle Pr between human and rodents predict similar short-term plasticity of transmission, a key feature of synapses of dynamic neuronal

networks, with an additional tuning range for human connection strength due to higher N_{FRS}.

How these efficient synapses are formed is unknown to date, however, the selective downregulation of the powerful pyramidal cell to interneuron synapses was reported in the human brain (Szegedi et al., 2016). The features of this long term depression are in line with our results showing MVR in these efficient excitatory synapses. The long term depression described by Szegedi et al. occurs only in the synaptic connenctions with large amplitudes, depends on the activation of metabotropic glutamate receptors, and the elevated activity of the presynaptic cell is sufficient for its generation. These results suggest that the amount of glutamate released from the multivesicular synapses during elevated presynaptic activity is so large that the glutamate can overcome the reuptake system and diffuse to extrasynaptic metabotropic glutamate receptors. One can hypothesize that during this form of long term depression the efficient MVR synapses transform to weak non-MVR synapses (Szegedi et al., 2016).

Our results provide an in depth understanding of the mechanisms underlying the powerful, unitary EPSP-evoked suprathreshold series of events in the human neocortex (Komlósi et al., 2012; Molnár et al., 2008; Szegedi et al., 2016; Szegedi et al., 2017), which might be an essential cellular component underlying the generation of Hebbian-like cell assemblies (Hebb, 1949). Even if upscaling of release components simply follows larger neurons and synapses in the human microcircuit, it is important to note that scalability of multivesicular release in human synapses (as opposed to all-or-none single vesicular rat synapses) provides additional functional variability, which might subserve evolutionary optimization. The strong connections linking pyramidal cells and a select group of postsynaptic neurons in the same area of the neocortex could be strategically positioned for the emergence and

maintenance of key cortical hubs characteristic of the human cerebral cortex (Hagmann et al., 2008). Long-range connections of PCs with strong local connections might also target distant interneurons with similarly powerful unitary EPSPs speculatively providing structural and functional basis for the formation of small world networks suggested to be important in linking connections to cognition (Park and Friston, 2013).

Acknowledgements

First of all, I would like to thank my supervisor, Gábor Tamás, for giving me the opportunity to work in his lab. The peaceful and at the same time stimulating environment he created is instrumental for high quality research. His questions, advices and torrent of ideas propelled our work throughout my university and doctorate years. I would like to thank the former and current members of the lab, for example Miklós Füle, Szabolcs Oláh, Gergely Komlósi and Gábor Molnár, who introduced me to the basics of electrophysiology and everyday lab routines. I would like to further thank Gábor Molnár who helped every step of mine throughout the years with technical support and fruitful scientific discussions. I would like to thank the co-authors of the publications this thesis is based on: Sándor Bordé for the work with the cell taxonomy algorithm, Judith Baka for her indispensable light- and electron microscopic work, Noémi Holderith and Zoltán Nusser for their electronmicroscopic expertise and Gábor Molnár for the work and help in the electrophysiological experiments. Furthermore, I would like to thank all the current lab members for the continuously stimulating and friendly atmosphere. Last, but not least I would like to thank the essential technical and administrative assistance to Éva Tóth, Margó Váradi, Nelli Tóth, Leóna Mezei and Bettina Lehóczki.

I feel deep gratitude towards my family: my wife Juci, my mother, brother and sister. Their support and love were great help in the desperate times of research.

Bibliography

Agnati, L. F. et al. (2006). "Volume transmission and wiring transmission from cellular to molecular networks: history and perspectives." In: *Acta Physiol. (Oxf).* 187.1-2, pp. 329–44. ISSN: 1748-1708. DOI: 10.1111/j.1748-1716.2006.01579.x.

Alfó, Marco, Luciano Nieddu, and Donatella Vicari (2009). "Finite mixture models for mapping spatially dependent disease counts." In: *Biom. J.* 51.1, pp. 84–97. ISSN: 1521-4036. DOI: 10.1002/bimj.200810494.

Amzica, Florin, Marcello Massimini, and Alfredo Manfridi (2002). "Spatial buffering during slow and paroxysmal sleep oscillations in cortical networks of glial cells in vivo." In: *J. Neurosci.* 22.3, pp. 1042–53. ISSN: 1529-2401.

Ballanyi, K, P Grafe, and G ten Bruggencate (1987). "Ion activities and potassium uptake mechanisms of glial cells in guinea-pig olfactory cortex slices." In: *J. Physiol.* 382, pp. 159–74. ISSN: 0022-3751. DOI: 10.1113/jphysiol.1987.sp016361.

Barbour, Boris and Michael Häusser (1997). "Intersynaptic diffusion of neurotransmitter." In: *Trends Neurosci.* 20.9, pp. 377–84. ISSN: 0166-2236. DOI: 10.1016/S0166-2236(96)20050-5.

Bergles, D E et al. (2000). "Glutamatergic synapses on oligodendrocyte precursor cells in the hippocampus." In: *Nature* 405.6783, pp. 187–91. ISSN: 0028-0836. DOI: 10.1038/35012083.

Biró, Agota, Noémi B Holderith, and Zoltan Nusser (2005). "Quantal size is independent of the release probability at hippocampal excitatory synapses." In: *J. Neurosci.* 25.1, pp. 223–32. ISSN: 1529-2401. DOI: 10.1523/JNEUROSCI.3688-04.2005.

Biró, Ágota, Noémi B Holderith, and Zoltan Nusser (2006). "Release probability-dependent scaling of the postsynaptic responses at single hippocampal GABAergic synapses." In: *J. Neurosci.* 26.48, pp. 12487–96. ISSN: 1529-2401. DOI: 10.1523/JNEUROSCI.3106-06.2006.

Bliss, T V and A R Gardner-Medwin (1973). "Long-lasting potentiation of synaptic transmission in the dentate area of the unanaestetized rabbit following stimulation of the perforant path." In: *J. Physiol.* 232.2, pp. 357–74. ISSN: 0022-3751.

Boddum, Kim et al. (2016). "Astrocytic GABA transporter activity modulates excitatory neurotransmission." In: *Nat. Commun.* 7, p. 13572. ISSN: 2041-1723. DOI: 10.1038/ncomms13572.

Boldog, Eszter et al. (2017). "Transcriptomic and morphophysiological evidence for a specialized human cortical {GABAergic} cell type". In: *bioRxiv*. DOI: 10.1101/216085.

Buhl, E H et al. (1994). "Physiological properties of anatomically identified axo-axonic cells in the rat hippocampus." In: *J. Neurophysiol.* 71.4, pp. 1289–307. ISSN: 0022-3077. DOI: 10.1152/jn.1994.71.4.1289.

Bushong, Eric A, Maryann E Martone, and Mark H Ellisman (2004). "Maturation of astrocyte morphology and the establishment of astrocyte domains during postnatal hippocampal development." In: *Int. J. Dev. Neurosci.* 22.2, pp. 73–86. ISSN: 0736-5748. DOI: 10.1016/j.ijdevneu.2003.12.008.

Bushong, Eric A et al. (2002). "Protoplasmic astrocytes in CA1 stratum radiatum occupy separate anatomical domains." In: *J. Neurosci.* 22.1, pp. 183–92. ISSN: 1529-2401.

Butt, Arthur and Alexei Verkhratsky (2013). *Glial Physiology and Pathophysiology*. ISBN: 9780470015643.

Buzsáki, György (2015). "Hippocampal sharp wave-ripple: A cognitive biomarker for episodic memory and planning". In: *Hippocampus* 25.10, pp. 1073–1188. ISSN: 10981063. DOI: 10.1002/hipo.22488. arXiv: arXiv:1011.1669v3.

Cahoy, John D et al. (2008). "A Transcriptome Database for Astrocytes, Neurons, and Oligodendrocytes: A New Resource for Understanding Brain Development and Function". In: *J. Neurosci.* 28.1, pp. 264–278. ISSN: 0270-6474. DOI: 10.1523/JNEUROSCI.4178-07.2008.

Capogna, Marco (2011). "Neurogliaform cells and other interneurons of stratum lacunosum-moleculare gate entorhinal-hippocampal dialogue." In: *J. Physiol.* 589.Pt 8, pp. 1875–83. ISSN: 1469-7793. DOI: 10.1113/jphysiol.2010.201004.

Capogna, Marco and Robert a Pearce (2011). "GABA A,slow: causes and consequences." In: *Trends Neurosci.* 34.2, pp. 101–12. ISSN: 1878-108X. DOI: 10.1016/j.tins.2010.10.005.

Castillo, J del and B Katz (1954). "Quantal components of the end-plate potential." In: *J. Physiol.* 124.3, pp. 560–73. ISSN: 0022-3751.

Cauli, B et al. (1997). "Molecular and physiological diversity of cortical nonpyramidal cells." In: *J. Neurosci.* 17.10, pp. 3894–906. ISSN: 0270-6474.

Chittajallu, Ramesh, Kenneth A Pelkey, and Chris J McBain (2013). "Neurogliaform cells dynamically regulate somatosensory integration via synapse-specific modulation." In: *Nat. Neurosci.* 16.1, pp. 13–5. ISSN: 1546-1726. DOI: 10.1038/nn.3284.

Clements, John D. and R A Silver (2000). "Unveiling synaptic plasticity: a new graphical and analytical approach." In: *Trends Neurosci.* 23.3, pp. 105–13. ISSN: 0166-2236. DOI: 10.1016/S0166-2236(99)01520-9.

Covelo, Ana and Alfonso Araque (2018). "Neuronal activity determines distinct gliotransmitter release from a single astrocyte." In: *Elife* 7, pp. 1–19. ISSN: 2050-084X. DOI: 10.7554/eLife.32237.

Craig, Michael T and Chris J McBain (2014). "The emerging role of GABAB receptors as regulators of network dynamics: fast actions from a 'slow' receptor?" In: *Curr. Opin. Neurobiol.* 26, pp. 15–21. ISSN: 1873-6882. DOI: 10.1016/j.conb.2013.10.002.

Craig, Michael T et al. (2013). "Distinct roles of GABAB1a- and GABAB1b-containing GABAB receptors in spontaneous and evoked termination of persistent cortical activity." In: *J. Physiol.* 591.Pt 4, pp. 835–43. ISSN: 1469-7793. DOI: 10.1113/jphysiol.2012.248088.

De Felipe, J et al. (1997). "Inhibitory synaptogenesis in mouse somatosensory cortex." In: *Cereb. Cortex* 7.7, pp. 619–34. ISSN: 1047-3211.

DeFelipe, J (1993). "Neocortical neuronal diversity: chemical heterogeneity revealed by colocalization studies of classic neurotransmitters, neuropeptides, calcium-binding proteins, and cell surface molecules." In: *Cereb. Cortex* 3.4, pp. 273–89. ISSN: 1047-3211.

Di Castro, Maria Amalia et al. (2011). "Local Ca2+ detection and modulation of synaptic release by astrocytes". In: *Nat. Neurosci.* 14.10, pp. 1276–1284. ISSN: 1097-6256. DOI: 10.1038/nn.2929.

Doengi, Michael et al. (2009). "GABA uptake-dependent Ca2+ signaling in developing olfactory bulb astrocytes". In: *Proc. Natl. Acad. Sci.* 106.41, pp. 17570–17575. ISSN: 0027-8424. DOI: 10.1073/pnas.0809513106.

Dy, Jennifer G and Carla E Brodley (2004). "Feature Selection for Unsupervised Learning". In: *J. Mach. Learn. Res.* 5, pp. 845–889. ISSN: 0395-3890.

Egawa, Kiyoshi et al. (2013). "Cl- homeodynamics in gap junction-coupled astrocytic networks on activation of GABAergic synapses." In: *J. Physiol.* 591.16, pp. 3901–17. ISSN: 1469-7793. DOI: 10.1113/jphysiol.2013.257162.

Eulenburg, Volker and Jesús Gomeza (2010). "Neurotransmitter transporters expressed in glial cells as regulators of synapse function." In: *Brain Res. Rev.* 63.1-2, pp. 103–12. ISSN: 1872-6321. DOI: 10.1016/j.brainresrev.2010.01.003.

Farrant, Mark and Zoltan Nusser (2005). "Variations on an inhibitory theme: phasic and tonic activation of GABAA receptors". In: *Nat. Rev. Neurosci.* 6.3, pp. 215–229. ISSN: 1471-003X. DOI: 10.1038/nrn1625.

Fiacco, Todd A. and Ken D. McCarthy (2018). "Multiple Lines of Evidence Indicate That Gliotransmission Does Not Occur under Physiological Conditions". In: *J. Neurosci.* 38.1, pp. 3–13. ISSN: 0270-6474. DOI: 10.1523/JNEUROSCI.0016-17.2017.

Freeman, Marc R (2010). "Specification and morphogenesis of astrocytes." In: *Science* 330.6005, pp. 774–8. ISSN: 1095-9203. DOI: 10.1126/science.1190928.

Freund, Tamás F. and István Katona (2007). "Perisomatic inhibition." In: *Neuron* 56.1, pp. 33–42. ISSN: 0896-6273. DOI: 10.1016/j.neuron.2007.09.012.

Freund, TF F and György Buzsáki (1996). "Interneurons of the hippocampus." In: *Hippocampus* 6.4, pp. 347–470. ISSN: 1050-9631. DOI: 10.1002/(SICI)1098-1063(1996)6:4<347::AID-HIPO1>3.0.CO;2-I.

Fricker, D and R Miles (2000). "EPSP amplification and the precision of spike timing in hippocampal neurons." In: *Neuron* 28.2, pp. 559–69. ISSN: 0896-6273.

Fritschy, Jean-Marc et al. (2004). "Independent maturation of the GABA(B) receptor subunits GABA(B1) and GABA(B2) during postnatal development in rodent

brain." In: *J. Comp. Neurol.* 477.3, pp. 235–52. ISSN: 0021-9967. DOI: 10.1002/cne.20188.

Galarreta, M and S Hestrin (2001). "Spike transmission and synchrony detection in networks of GABAergic interneurons." In: *Science* 292.5525, pp. 2295–9. ISSN: 0036-8075. DOI: 10.1126/science.1061395.

Ge, Woo Ping et al. (2012). "Local generation of glia is a major astrocyte source in postnatal cortex". In: *Nature* 484.7394, pp. 376–380. ISSN: 00280836. DOI: 10.1038/nature10959.

Gentet, Luc J. et al. (2010). "Membrane potential dynamics of GABAergic neurons in the barrel cortex of behaving mice." In: *Neuron* 65.3, pp. 422–35. ISSN: 1097-4199. DOI: 10.1016/j.neuron.2010.01.006.

Grosche, J et al. (1999). "Microdomains for neuron-glia interaction: parallel fiber signaling to Bergmann glial cells." In: *Nat. Neurosci.* 2.2, pp. 139–43. ISSN: 1097-6256. DOI: 10.1038/5692.

Gulyás, A I et al. (1993). "Hippocampal pyramidal cells excite inhibitory neurons through a single release site." In: *Nature* 366.6456, pp. 683–7. ISSN: 0028-0836. DOI: 10.1038/366683a0.

Gupta, A., Y Wang, and H Markram (2000). "Organizing principles for a diversity of GABAergic interneurons and synapses in the neocortex." In: *Science* 287.5451, pp. 273–8. ISSN: 0036-8075. DOI: 10.1126/science.287.5451.273.

Hagmann, Patric et al. (2008). "Mapping the structural core of human cerebral cortex." In: *PLoS Biol.* 6.7. Ed. by Karl J Friston, e159. ISSN: 1545-7885. DOI: 10.1371/journal.pbio.0060159.

Hebb, D O (1949). *The organization of behavior*. New York: Wiley & Sons.

Hendry, S H and E G Jones (1985). "Morphology of synapses formed by cholecystokinin-immunoreactive axon terminals in regio superior of rat hippocampus." In: *Neuroscience* 16.1, pp. 57–68. ISSN: 0306-4522.

Hibino, Hiroshi et al. (2010). "Inwardly rectifying potassium channels: their structure, function, and physiological roles." In: *Physiol. Rev.* 90.1, pp. 291–366. ISSN: 1522-1210. DOI: 10.1152/physrev.00021.2009.

Hille, Bertil (1992). *Ionic Channels in Excitable membranes*, p. 607.

Holderith, Noemi et al. (2012). "Release probability of hippocampal glutamatergic terminals scales with the size of the active zone." In: *Nat. Neurosci.* 15.7, pp. 988–97. ISSN: 1546-1726. DOI: 10.1038/nn.3137.

Ishikawa, Taro, Yoshinori Sahara, and Tomoyuki Takahashi (2002). "A single packet of transmitter does not saturate postsynaptic glutamate receptors." In: *Neuron* 34.4, pp. 613–21. ISSN: 0896-6273. DOI: 10.1016/S0896-6273(02)00692-X.

Jiang, Xiaolong et al. (2015). "Principles of connectivity among morphologically defined cell types in adult neocortex." In: *Science* 350.6264, aac9462. ISSN: 1095-9203. DOI: 10.1126/science.aac9462.

Kaila, K et al. (1997). "Long-lasting GABA-mediated depolarization evoked by high-frequency stimulation in pyramidal neurons of rat hippocampal slice is attributable to a network-driven, bicarbonate-dependent K+ transient." In: *J. Neurosci.* 17.20, pp. 7662–72. ISSN: 0270-6474.

Kang, J et al. (1998). "Astrocyte-mediated potentiation of inhibitory synaptic transmission." In: *Nat. Neurosci.* 1.8, pp. 683–92. ISSN: 1097-6256. DOI: 10.1038/3684.

Katona, Gergely et al. (2012). "Fast two-photon in vivo imaging with three-dimensional random-access scanning in large tissue volumes". In: *Nat. Methods* 9.2, pp. 201–208. ISSN: 1548-7091. DOI: 10.1038/nmeth.1851.

Katz, Bernard (1969). *The release of neural transmitter substances*.

Kaupmann, K et al. (1997). "Expression cloning of GABA(B) receptors uncovers similarity to metabotropic glutamate receptors." In: *Nature* 386.6622, pp. 239–46. ISSN: 0028-0836. DOI: 10.1038/386239a0.

Kawaguchi, Y (1993). "Groupings of nonpyramidal and pyramidal cells with specific physiological and morphological characteristics in rat frontal cortex." In: *J. Neurophysiol.* 69.2, pp. 416–31. ISSN: 0022-3077. DOI: 10.1152/jn.1993.69.2.416.

Kawaguchi, Y and Y Kubota (1996). "Physiological and morphological identification of somatostatin- or vasoactive intestinal polypeptide-containing cells among GABAergic cell subtypes in rat frontal cortex." In: *J. Neurosci.* 16.8, pp. 2701–15. ISSN: 0270-6474.

Kawaguchi, Yasuo and Y Kubota (1997). "GABAergic cell subtypes and their synaptic connections in rat frontal cortex." In: *Cereb. Cortex* 7.6, pp. 476–86. ISSN: 1047-3211. DOI: 10.1093/cercor/7.6.476.

Kepecs, Adam and Gordon Fishell (2014). "Interneuron cell types are fit to function." In: *Nature* 505, pp. 318–26. ISSN: 1476-4687. DOI: 10.1038/nature12983.

Kettenmann, H, K H Backus, and M Schachner (1984). "Aspartate, glutamate and gamma-aminobutyric acid depolarize cultured astrocytes." In: *Neurosci. Lett.* 52.1-2, pp. 25–9. ISSN: 0304-3940. DOI: 10.1016/0304-3940(84)90345-8.

Kisvárday, Z F, C Beaulieu, and U T Eysel (1993). "Network of GABAergic large basket cells in cat visual cortex (area 18): implication for lateral disinhibition." In: *J. Comp. Neurol.* 327.3, pp. 398–415. ISSN: 0021-9967. DOI: 10.1002/cne.903270307.

Klausberger, Thomas and Peter Somogyi (2008). "Neuronal Diversity and Temporal Dynamics: The Unity of Hippocampal Circuit Operations". In: *Science (80-.).* 321.5885, pp. 53–57. ISSN: 0036-8075. DOI: 10.1126/science.1149381.

Kofuji, P and E a Newman (2004). "Potassium buffering in the central nervous system." In: *Neuroscience* 129.4, pp. 1045–56. ISSN: 0306-4522. DOI: 10.1016/j.neuroscience.2004.06.008.

Komlósi, Gergely et al. (2012). "Fluoxetine (prozac) and serotonin act on excitatory synaptic transmission to suppress single layer 2/3 pyramidal neuron-triggered cell assemblies in the human prefrontal cortex." In: *J. Neurosci.* 32.46, pp. 16369–78. ISSN: 1529-2401. DOI: 10.1523/JNEUROSCI.2618-12.2012.

Korn, H et al. (1982). "Transmission at a central inhibitory synapse. II. Quantal description of release, with a physical correlate for binomial n." In: *J. Neurophysiol.* 48.3, pp. 679–707. ISSN: 0022-3077. DOI: 10.1152/jn.1982.48.3.679.

Lee, Sang-Hun, Csaba Földy, and Ivan Soltesz (2010). "Distinct endocannabinoid control of GABA release at perisomatic and dendritic synapses in the hippocampus." In: *J. Neurosci.* 30.23, pp. 7993–8000. ISSN: 1529-2401. DOI: 10.1523/JNEUROSCI.6238-09.2010.

Li, Yuanhong, Ming Dong, and Jing Hua (2008). "Localized feature selection for clustering". In: *Pattern Recognit. Lett.* 29.1, pp. 10–18. ISSN: 01678655. DOI: 10.1016/j.patrec.2007.08.012.

Lin, Shih-chun and Dwight E Bergles (2004). "Synaptic signaling between GABAergic interneurons and oligodendrocyte precursor cells in the hippocampus." In: *Nat. Neurosci.* 7.1, pp. 24–32. ISSN: 1097-6256. DOI: 10.1038/nn1162.

López-Bendito, Guillermina et al. (2004). "Distribution of metabotropic GABA receptor subunits GABAB1a/b and GABAB2 in the rat hippocampus during prenatal and postnatal development." In: *Hippocampus* 14.7, pp. 836–48. ISSN: 1050-9631. DOI: 10.1002/hipo.10221.

Losi, Gabriele, Letizia Mariotti, and Giorgio Carmignoto (2014). "GABAergic interneuron to astrocyte signalling: a neglected form of cell communication in the brain." In: *Philos. Trans. R. Soc. Lond. B. Biol. Sci.* 369.1654, p. 20130609. ISSN: 1471-2970. DOI: 10.1098/rstb.2013.0609.

Luján, R and R Shigemoto (2006). "Localization of metabotropic GABA receptor subunits GABAB1 and GABAB2 relative to synaptic sites in the rat developing cerebellum". In: *Eur. J. Neurosci.* 23.6, pp. 1479–1490. ISSN: 0953816X. DOI: 10.1111/j.1460-9568.2006.04669.x.

Lund, R D and Jennifer S. Lund (1972). "Development of synaptic patterns in the superior colliculus of the rat." In: *Brain Res.* 42.1, pp. 1–20. ISSN: 0006-8993. DOI: 10.1016/0042-6989(71)90046-0.

Ma, Bao-Feng, Min-Jie Xie, and Min Zhou (2012). "Bicarbonate efflux via GABAA receptors depolarizes membrane potential and inhibits two-pore domain potassium channels of astrocytes in rat hippocampal slices". In: *Glia* 60.11, pp. 1761–1772. ISSN: 08941491. DOI: 10.1002/glia.22395.

Ma, Baofeng et al. (2014). "Dual patch voltage clamp study of low membrane resistance astrocytes in situ." In: *Mol. Brain* 7.1, p. 18. ISSN: 1756-6606. DOI: 10.1186/1756-6606-7-18.

Maccaferri, G et al. (2000). "Cell surface domain specific postsynaptic currents evoked by identified GABAergic neurones in rat hippocampus in vitro." In: *J. Physiol.* 524 Pt 1, pp. 91–116. ISSN: 0022-3751.

Maldonado, Paloma P and María Cecilia Angulo (2015). "Multiple Modes of Communication between Neurons and Oligodendrocyte Precursor Cells." In: *Neuroscientist* 21.3, pp. 266–76. ISSN: 1089-4098. DOI: 10.1177/1073858414530784.

Mann, Edward O, Michael M Kohl, and Ole Paulsen (2009). "Distinct Roles of GABAA and GABAB Receptors in Balancing and Terminating Persistent Cortical Activity". In: *J. Neurosci.* 29.23, pp. 7513–7518. ISSN: 0270-6474. DOI: 10.1523/JNEUROSCI.6162-08.2009.

Mariotti, Letizia et al. (2018). "Interneuron-specific signaling evokes distinctive somatostatin-mediated responses in adult cortical astrocytes." In: *Nat. Commun.* 9.1, p. 82. ISSN: 2041-1723. DOI: 10.1038/s41467-017-02642-6.

Markram, Henry et al. (2004). "Interneurons of the neocortical inhibitory system". In: *Nat. Rev. Neurosci.* 5.10, pp. 793–807. ISSN: 1471-003X. DOI: 10.1038/nrn1519.

Markram, Henry et al. (2015). "Reconstruction and Simulation of Neocortical Microcircuitry". In: *Cell* 163.2, pp. 456–492. ISSN: 10974172. DOI: 10.1016/j.cell.2015.09.029.

Martin, Stella C et al. (2004). "Differential expression of gamma-aminobutyric acid type B receptor subunit mRNAs in the developing nervous system and receptor coupling to adenylyl cyclase in embryonic neurons." In: *J. Comp. Neurol.* 473.1, pp. 16–29. ISSN: 0021-9967. DOI: 10.1002/cne.20094.

Matyash, Vitali and Helmut Kettenmann (2010). "Heterogeneity in astrocyte morphology and physiology." In: *Brain Res. Rev.* 63.1-2, pp. 2–10. ISSN: 1872-6321. DOI: 10.1016/j.brainresrev.2009.12.001.

McCormick, D a et al. (1985). "Comparative electrophysiology of pyramidal and sparsely spiny stellate neurons of the neocortex". In: *J Neurophysiol* 54.4, pp. 782–806. ISSN: 0022-3077.

Meier, Silke D, Karl W Kafitz, and Christine R Rose (2008). "Developmental profile and mechanisms of GABA-induced calcium signaling in hippocampal astrocytes". In: *Glia* 56.10, pp. 1127–1137. ISSN: 08941491. DOI: 10.1002/glia.20684.

Miles, R and R K Wong (1984). "Unitary inhibitory synaptic potentials in the guinea-pig hippocampus in vitro." In: *J. Physiol.* 356, pp. 97–113. ISSN: 0022-3751.

Miles, Richard and R K Wong (1986). "Excitatory synaptic interactions between CA3 neurones in the guinea-pig hippocampus." In: *J. Physiol.* 373, pp. 397–418. ISSN: 0022-3751.

Mishima, Tsuneko and Hajime Hirase (2010). "In Vivo Intracellular Recording Suggests That Gray Matter Astrocytes in Mature Cerebral Cortex and Hippocampus Are Electrophysiologically Homogeneous". In: *J. Neurosci.* 30.8, pp. 3093–3100. ISSN: 0270-6474. DOI: 10.1523/JNEUROSCI.5065-09.2010.

Mohan, Hemanth et al. (2015). "Dendritic and Axonal Architecture of Individual Pyramidal Neurons across Layers of Adult Human Neocortex." In: *Cereb. Cortex* 25.12, pp. 4839–53. ISSN: 1460-2199. DOI: 10.1093/cercor/bhv188.

Molnár, Gábor et al. (2008). "Complex events initiated by individual spikes in the human cerebral cortex." In: *PLoS Biol.* 6.9. Ed. by Rafael Yuste, e222. ISSN: 1545-7885. DOI: 10.1371/journal.pbio.0060222.

Neher, Erwin (2010). "What is Rate-Limiting during Sustained Synaptic Activity: Vesicle Supply or the Availability of Release Sites." In: *Front. Synaptic Neurosci.* 2, p. 144. ISSN: 1663-3563. DOI: 10.3389/fnsyn.2010.00144.

Nilsson, M et al. (1993). "GABA induces Ca2+ transients in astrocytes." In: *Neuroscience* 54.3, pp. 605–614. ISSN: 03064522. DOI: 10.1016/0306-4522(93)90232-5.

Ogata, Katuya and T. Kosaka (2002). "Structural and quantitative analysis of astrocytes in the mouse hippocampus." In: *Neuroscience* 113.1, pp. 221–33. ISSN: 0306-4522. DOI: 10.1016/S0306-4522(02)00041-6.

Oláh, Szabolcs et al. (2007). "Output of neurogliaform cells to various neuron types in the human and rat cerebral cortex." In: *Front. Neural Circuits* 1.November, p. 4. ISSN: 1662-5110. DOI: 10.3389/neuro.04.004.2007.

Oláh, Szabolcs et al. (2009). "Regulation of cortical microcircuits by unitary GABA-mediated volume transmission." In: *Nature* 461.7268, pp. 1278–1281. ISSN: 0028-0836. DOI: 10.1038/nature08503.

Oldfield, Claire S., Alain Marty, and Brandon M. Stell (2010). "Interneurons of the cerebellar cortex toggle Purkinje cells between up and down states". In: *Proc. Natl. Acad. Sci.* 107.29, pp. 13153–13158. ISSN: 0027-8424. DOI: 10.1073/pnas.1002082107.

Otis, T S, K J Staley, and I Mody (1991). "Perpetual inhibitory activity in mammalian brain slices generated by spontaneous GABA release." In: *Brain Res.* 545.1-2, pp. 142–50. ISSN: 0006-8993.

Overstreet-Wadiche, Linda and Chris J. McBain (2015). "Neurogliaform cells in cortical circuits." In: *Nat. Rev. Neurosci.* 16.8, pp. 458–68. ISSN: 1471-0048. DOI: 10.1038/nrn3969.

Park, Hae-Jeong and Karl Friston (2013). "Structural and functional brain networks: from connections to cognition." In: *Science* 342.6158, p. 1238411. ISSN: 1095-9203. DOI: 10.1126/science.1238411.

Pawelzik, H et al. (1999). *Modulation of bistratified cell IPSPs and basket cell IPSPs by pentobarbitone sodium, diazepam and Zn2+: dual recordings in slices of adult rat hippocampus*.

Perea, Gertrudis et al. (2016). "Activity-dependent switch of GABAergic inhibition into glutamatergic excitation in astrocyte-neuron networks." In: *Elife* 5.DECEMBER2016, pp. 1–26. ISSN: 2050-084X. DOI: 10.7554/eLife.20362.

Péterfi, Zoltán et al. (2012). "Endocannabinoid-mediated long-term depression of afferent excitatory synapses in hippocampal pyramidal cells and GABAergic interneurons." In: *J. Neurosci.* 32.41, pp. 14448–63. ISSN: 1529-2401. DOI: 10.1523/JNEUROSCI.1676-12.2012.

Peters, A, R L Saint Marie, and A / Jones Peters E. G. (1984). *Smooth and sparsely spinous nonpyramidal cells forming local axonal plexuses.* Vol. 1. New York: Plenum Press.

Porter, J T and K D McCarthy (1997). "Astrocytic neurotransmitter receptors in situ and in vivo." In: *Prog. Neurobiol.* 51.4, pp. 439–55. ISSN: 0301-0082. DOI: 10.1016/S0301-0082(96)00068-8.

Pouille, Frédéric and Massimo Scanziani (2004). "Routing of spike series by dynamic circuits in the hippocampus". In: *Nature* 429.6993, pp. 717–723. ISSN: 0028-0836. DOI: 10.1038/nature02615.

Prince, David A. and R K Wong (1981). "Human epileptic neurons studied in vitro." In: *Brain Res.* 210.1-2, pp. 323–33. ISSN: 0006-8993. DOI: 10.1016/0006-8993(81)90905-7.

Pulido, Camila et al. (2015). "Vesicular release statistics and unitary postsynaptic current at single GABAergic synapses." In: *Neuron* 85.1, pp. 159–72. ISSN: 1097-4199. DOI: 10.1016/j.neuron.2014.12.006.

Roth, Gerhard and Ursula Dicke (2005). "Evolution of the brain and intelligence." In: *Trends Cogn. Sci.* 9.5, pp. 250–7. ISSN: 1364-6613. DOI: 10.1016/j.tics.2005.03.005.

Rudolph, Stephanie et al. (2015). "The ubiquitous nature of multivesicular release." In: *Trends Neurosci.* 38.7, pp. 428–38. ISSN: 1878-108X. DOI: 10.1016/j.tins.2015.05.008.

Sakaba, Takeshi, Ralf Schneggenburger, and Erwin Neher (2002). "Estimation of quantal parameters at the calyx of Held synapse." In: *Neurosci. Res.* 44.4, pp. 343–56. ISSN: 0168-0102.

Sauvageot, Claire M. and Charles D. Stiles (2002). "Molecular mechanisms controlling cortical gliogenesis". In: *Curr. Opin. Neurobiol.* 12.3, pp. 244–249. ISSN: 09594388. DOI: 10.1016/S0959-4388(02)00322-7.

Saviane, Chiara and R. Angus Silver (2007). "Estimation of quantal parameters with multiple-probability fluctuation analysis." In: *Methods Mol. Biol.* 403, pp. 303–17. ISSN: 1064-3745. DOI: 10.1007/978-1-59745-529-9_19.

Savtchouk, Iaroslav and Andrea Volterra (2018). "Gliotransmission: Beyond Black-and-White". In: *J. Neurosci.* 38.1, pp. 14–25. ISSN: 0270-6474. DOI: 10.1523/JNEUROSCI.0017-17.2017.

Scheuss, Volker, Ralf Schneggenburger, and Erwin Neher (2002). "Separation of presynaptic and postsynaptic contributions to depression by covariance analysis of successive EPSCs at the calyx of Held synapse." In: *J. Neurosci.* 22.3, pp. 728–39. ISSN: 1529-2401. DOI: 22/3/728[pii].

Schwartzkroin, P A and W D Knowles (1984). "Intracellular study of human epileptic cortex: in vitro maintenance of epileptiform activity?" In: *Science* 223.4637, pp. 709–12. ISSN: 0036-8075.

Serrano, Alexandre et al. (2006). "GABAergic network activation of glial cells underlies hippocampal heterosynaptic depression." In: *J. Neurosci.* 26.20, pp. 5370–5382. ISSN: 1529-2401. DOI: 10.1523/JNEUROSCI.5255-05.2006.

Silver, R a, a Momiyama, and S G Cull-Candy (1998). "Locus of frequency-dependent depression identified with multiple-probability fluctuation analysis at rat climbing fibre-Purkinje cell synapses." In: *J. Physiol.* 510 (Pt 3, pp. 881–902. ISSN: 0022-3751. DOI: 10.1111/j.1469-7793.1998.881bj.x.

Silver, R Angus (2003). "Estimation of nonuniform quantal parameters with multiple-probability fluctuation analysis: theory, application and limitations." In: *J. Neurosci. Methods* 130.2, pp. 127–41. ISSN: 0165-0270. DOI: 10.1016/j.jneumeth.2003.09.030.

Simon, Anna et al. (2005). "Gap-junctional coupling between neurogliaform cells and various interneuron types in the neocortex." In: *J. Neurosci.* 25.27, pp. 6278–85. ISSN: 1529-2401. DOI: 10.1523/JNEUROSCI.1431-05.2005.

Singer, Wolf (1995). "Development and plasticity of cortical processing architectures." In: *Science* 270.5237, pp. 758–64. ISSN: 0036-8075.

Sloan, Steven A and Ben A Barres (2014). "Looks can be deceiving: reconsidering the evidence for gliotransmission." In: *Neuron* 84.6, pp. 1112–5. ISSN: 1097-4199. DOI: 10.1016/j.neuron.2014.12.003.

Somogyi, P (1977). "A specific 'axo-axonal' interneuron in the visual cortex of the rat." In: *Brain Res.* 136.2, pp. 345–50. ISSN: 0006-8993.

Somogyi, P et al. (1983). "Synaptic connections of morphologically identified and physiologically characterized large basket cells in the striate cortex of cat." In: *Neuroscience* 10.2, pp. 261–94. ISSN: 0306-4522.

Somogyi, P et al. (1998). "Salient features of synaptic organisation in the cerebral cortex." In: *Brain Res. Brain Res. Rev.* 26.2-3, pp. 113–35.

Spruston, Nelson (2008). "Pyramidal neurons: dendritic structure and synaptic integration." In: *Nat. Rev. Neurosci.* 9.3, pp. 206–21. ISSN: 1471-0048. DOI: 10.1038/nrn2286.

Sun, Wei et al. (2013). "Glutamate -Dependent Neuroglial Calcium Signaling Differs Between Young and Adult Brain". In: *Science (80-.).* 339.6116, pp. 197–200. ISSN: 0036-8075. DOI: 10.1126/science.1226740.Glutamate-Dependent.

Szabadics, János et al. (2006). "Excitatory effect of GABAergic axo-axonic cells in cortical microcircuits." In: *Science* 311.5758, pp. 233–5. ISSN: 1095-9203. DOI: 10.1126/science.1121325.

Szegedi, Viktor et al. (2016). "Plasticity in Single Axon Glutamatergic Connection to GABAergic Interneurons Regulates Complex Events in the Human Neocortex." In: *PLoS Biol.* 14.11, e2000237. ISSN: 1545-7885. DOI: 10.1371/journal.pbio.2000237.

Szegedi, Viktor et al. (2017). "High-Precision Fast-Spiking Basket Cell Discharges during Complex Events in the Human Neocortex." In: *eNeuro* 4.5, ENEURO.0260–17.2017. ISSN: 2373-2822. DOI: 10.1523/ENEURO.0260-17.2017.

Tamás, Gábor et al. (2003). "Identified sources and targets of slow inhibition in the neocortex." In: *Science* 299.5614, pp. 1902–1905. ISSN: 00368075. DOI: 10.1126/science.1082053.

Tasic, Bosiljka et al. (2016). "Adult mouse cortical cell taxonomy revealed by single cell transcriptomics". In: *Nat. Neurosci.* 19.2, pp. 335–346. ISSN: 1097-6256. DOI: 10.1038/nn.4216.

Tasic, Bosiljka et al. (2017). "Shared and distinct transcriptomic cell types across neocortical areas". In: *Biorxiv*. DOI: 10.1101/229542.

Thomson, Alex M et al. (2002). "Target and temporal pattern selection at neocortical synapses". In: *Philos. Trans. R. Soc. B Biol. Sci.* 357.1428, pp. 1781–1791. ISSN: 0962-8436. DOI: 10.1098/rstb.2002.1163.

Tremblay, Robin, Soohyun Lee, and Bernardo Rudy (2016). "GABAergic Interneurons in the Neocortex: From Cellular Properties to Circuits." In: *Neuron* 91.2, pp. 260–92. ISSN: 1097-4199. DOI: 10.1016/j.neuron.2016.06.033.

Vélez-Fort, Mateo, Etienne Audinat, and María Cecilia Angulo (2012). "Central role of GABA in neuron-glia interactions." In: *Neuroscientist* 18.3, pp. 237–50. ISSN: 1089-4098. DOI: 10.1177/1073858411403317.

Verhoog, Matthijs B et al. (2013). "Mechanisms underlying the rules for associative plasticity at adult human neocortical synapses." In: *J. Neurosci.* 33.43, pp. 17197–208. ISSN: 1529-2401. DOI: 10.1523/JNEUROSCI.3158-13.2013.

Viitanen, Tero et al. (2010). "The K+-Cl cotransporter KCC2 promotes GABAergic excitation in the mature rat hippocampus." In: *J. Physiol.* 588.Pt 9, pp. 1527–40. ISSN: 1469-7793. DOI: 10.1113/jphysiol.2009.181826.

Vizi, E Sylvester and Janos P Kiss (1998). "Neurochemistry and pharmacology of the major hippocampal transmitter systems: synaptic and nonsynaptic interactions." In: *Hippocampus* 8.6, pp. 566–607. ISSN: 1050-9631. DOI: 10.1002/(SICI)1098-1063(1998)8:6<566::AID-HIPO2>3.0.CO;2-W.

Vizi, E.Sylvester, Janos P. Kiss, and Balazs Lendvai (2004). "Nonsynaptic communication in the central nervous system". In: *Neurochem. Int.* 45.4, pp. 443–451. ISSN: 01970186. DOI: 10.1016/j.neuint.2003.11.016.

Volterra, Andrea, Nicolas Liaudet, and Iaroslav Savtchouk (2014). "Astrocyte Ca2+ signalling: an unexpected complexity". In: *Nat. Rev. Neurosci.* 15.5, pp. 327–335. ISSN: 1471-003X. DOI: 10.1038/nrn3725.

Wadiche, J I and C E Jahr (2001). "Multivesicular release at climbing fiber-Purkinje cell synapses." In: *Neuron* 32.2, pp. 301–13. ISSN: 0896-6273.

Wang, Bo et al. (2015). "A Subtype of Inhibitory Interneuron with Intrinsic Persistent Activity in Human and Monkey Neocortex." In: *Cell Rep.* Pp. 1–9. ISSN: 2211-1247. DOI: 10.1016/j.celrep.2015.02.018.

Wang, Fushun et al. (2012). "Bergmann glia modulate cerebellar Purkinje cell bistability via Ca2+-dependent K+ uptake." In: *Proc. Natl. Acad. Sci. U. S. A.* 109.20, pp. 7911–6. ISSN: 1091-6490. DOI: 10.1073/pnas.1120380109.

Warton, S S and R McCart (1989). "Synaptogenesis in the stratum griseum superficiale of the rat superior colliculus." In: *Synapse* 3.2, pp. 136–48. ISSN: 0887-4476. DOI: 10.1002/syn.890030205.

Williams, Stephen R and Simon J Mitchell (2008). "Direct measurement of somatic voltage clamp errors in central neurons." In: *Nat. Neurosci.* 11.7, pp. 790–8. ISSN: 1097-6256. DOI: 10.1038/nn.2137.

Woodruff, Alan and Rafael Yuste (2008). "Of mice and men, and chandeliers." In: *PLoS Biol.* 6.9, e243. ISSN: 1545-7885. DOI: 10.1371/journal.pbio.0060243.

Woodruff, Alan et al. (2009). "Depolarizing effect of neocortical chandelier neurons." In: *Front. Neural Circuits* 3.October, p. 15. ISSN: 1662-5110. DOI: 10.3389/neuro.04.015.2009.

Woodruff, Alan R. et al. (2011). "State-dependent function of neocortical chandelier cells." In: *J. Neurosci.* 31.49, pp. 17872–86. ISSN: 1529-2401. DOI: 10.1523/JNEUROSCI.3894-11.2011.

Yáñez, Inmaculada Ballesteros et al. (2005). "Double bouquet cell in the human cerebral cortex and a comparison with other mammals." In: *J. Comp. Neurol.* 486.4, pp. 344–60. ISSN: 0021-9967. DOI: 10.1002/cne.20533.

Zeisel, Amit et al. (2015). "Brain structure. Cell types in the mouse cortex and hippocampus revealed by single-cell RNA-seq." In: *Science* 347.6226, pp. 1138–42. ISSN: 1095-9203. DOI: 10.1126/science.aaa1934.

Zhang, Y. et al. (2014). "An RNA-Sequencing Transcriptome and Splicing Database of Glia, Neurons, and Vascular Cells of the Cerebral Cortex". In: *J. Neurosci.* 34.36, pp. 11929–11947. ISSN: 0270-6474. DOI: 10.1523/JNEUROSCI.1860-14.2014.

Zhang, Ye and Ben A Barres (2010). "Astrocyte heterogeneity: an underappreciated topic in neurobiology." In: *Curr. Opin. Neurobiol.* 20.5, pp. 588–94. ISSN: 1873-6882. DOI: 10.1016/j.conb.2010.06.005.

Zhou, Min (2005). "Development of GLAST(+) Astrocytes and NG2(+) Glia in Rat Hippocampus CA1: Mature Astrocytes Are Electrophysiologically Passive". In: *J. Neurophysiol.* 95.1, pp. 134–143. ISSN: 0022-3077. DOI: 10.1152/jn.00570.2005.

7 Abstract

The neocortex is the evolutionarily youngest part of the cerebral cortex and at the same time considered to be one of the most complex biological structures. Besides its crucial role in sensory perception and motor execution, this organ makes humans capable of performing sophisticated cognitive tasks. These cognitive abilities make neuroscientists so eager –and able– to decipher the workings of the human brain. Although the ultimate goal of neuroscience is to solve the human brain, most of the research is currently devoted to understanding the nervous system of simpler and more available model organisms, such as rodents', which still proves to be quite ambitious a task. The two most prominent cell types of the human brain are the neuronal and the glial cells. Glial cells are the major class of non-excitable cells in the brain. Among glia, astrocytes are the most extensively studied due to the fact that they comprise the most abundant and diverse glia class. Despite their diversity, their functions are shared: they are crucial for the extracellular ionic homeostasis, neurotransmitter uptake, synapse formation, regulation of blood–brain-barrier, and the development of the nervous system. The cortical neurons can be divided in two main groups: the excitatory projecting pyramidal cells and the inhibitory local interneurons. The local GABAergic interneurons constitute the minor fraction of neurons in the neocortex (10–20 %) but are instrumental for normal brain function. Despite their small numbers, these interneurons display extremely diverse morphological, electrophysiological and molecular properties. Our research group focuses

on the function, input and output of various interneuron types in the human and rodent neocortex.

In my doctorate study, we examined two very distinct synaptic connections. First, the output of a unique inhibitory interneuron, the neurogliaform cell (NGFCs). These GABAergic neurons were suggested to specialize in acting on GABA receptors on compartments of the neuronal surface which do not receive synaptic junctions, through a unitary form of volume transmission. The GABA released via volume transmission can effectively reach the extrasynaptic $GABA_A$ and $GABA_B$ receptors on virtually all neuronal processes within the axonal cloud of the NGFC. In the same vein, we hypothesized that neurogliaform interneurons might act on non-neuronal elements of the surrounding cortical tissue without establishing synaptic contacts. In my doctorate study, we show that there is a cell type selective unitary transmission from NGFCs to astrocytes with an early, $GABA_A$ receptor and GABA transporter-mediated component and a late component that results from the activation of GABA transporters and neuronal $GABA_B$ receptors. We could not detect Ca^{2+} influx in astrocytes associated with unitary GABAergic responses. Our experiments identify a presynaptic cell-type-specific, GABA-mediated communication pathway from individual neurons to astrocytes, assigning a role for unitary volume transmission in the control of ionic and neurotransmitter homeostasis.

In the second part of my work, we compared a ubiquitous excitatory synaptic connection between the human and the rat because classic theories link cognitive abilities to synaptic properties and human-specific biophysical features of synapses might contribute to the unparalleled performance of the human cerebral cortex. We performed paired recordings and multiple probability fluctuation analysis in pyramidal cell to basket cell synaptic connections in acute slice preparation from both

species. These experiments revealed similar quantal sizes, but four times more functional release sites in human pyramidal cell to fast-spiking interneuron connections compared to rats. These connections were mediated on average by three synaptic contacts in both species. Each presynaptic active zone contains 6.2 release sites in human, but only 1.6 in rats. Electron microscopy and electron microscopic tomography showed that an active zone harbors 4 docked vesicles in human, but only a single one in rats. Our results reveal a robust difference in the biophysical properties of a well-defined synaptic connection of the cortical microcircuit of human and rodents.

Our research had two main conclusions. First, we discovered of a novel interneuron-to-astrocyte signalling pathway, the function of which is probably to stabilize the widespread inhibitory action of neurogliaform interneurons through unitary GABAergic volume transmission. And second, we compared a ubiquitous synaptic connection in the human and rodent neocortex and found the biophysical differences in their workings that make human synapses more efficient.

8 Összefoglaló

Az agykéreg a sejtes szerveződés legkomplexebb struktúrája. Összetettségére utalnak bonyolult funkciói, melyek közül legfontosabbak az érzékelési, mozgási, és kognitív folyamatok szervezése. Az agyban található két fő sejttípus, a neuron és a glia közül a glia sejtek fordulnak elő nagyobb számban. A glia sejtek közül is a leggyakoribbak az asztrociták, melyek funkciói többek között az ionikus és metabolikus homeosztázis fenntartása. Az agykéreg leginkább kutatott idegsejtjei a projekciós, serkentő piramis sejtek, melyek az agykérgi idegsejtek viszonylag homogén, döntő többségét alkotják. Az agykéreg gátló sejtjei képzik az idegsejtek jóval diverzebb kisebbségét, melyek funkcionálisan is heterogénebbek, de minden esetben a serkentő többség működését szabályozzák. Kutatócsoportunk a humán és a rágcsáló agykéregben található gátló idegsejt altípusok felépítését és működését vizsgálja.

Doktori munkám során két jelentősen eltérően működő szinaptikus kapcsolatot vettünk górcső alá. Először az egyik agykéregben található gátló idegsejt típus, a neurogliaform sejt szinaptikus kimenetét vizsgáltuk. Kutatócsoportunk a közelmúltban megmutatta, hogy a neurogliaform sejt - egyedülálló módon az agykérgi sejtek között - képes lassú gátlás kialakítására. Sűrű axonarborizációja révén térfogati transzmisszióval árasztja el gátló neurotranszmitterrel (GABA) a környező neuronokat. A felszabadult GABA nem csak a szinaptikus résbe, hanem főként az extracelluláris térbe kerül, ahol szinaptikus és extraszinaptikus GABA receptorokat is aktivál. Doktori munkám során megmutatjuk, hogy a neurogliaform sejt egyetlen

akciós potenciálja hatására felszabaduló GABA hatással van a környező asztrocitákra is. A felszabaduló GABA direkt módon eléri az asztrociták ionotróp $GABA_A$ receptorait valamint GABA transzportereit és egy viszonylag gyors bemenő áramot generál, továbbá indirekt módon –neuronális metabotróp $GABAB_B$ receptorokon és klorid ion transzportereken keresztül– megemeli az extracelluláris tér kálium ion koncentrációját, mely egy lassú bemenő áramként detektálható a környező asztrocitákon. Kísérleteink azt mutatják, hogy a neurogliaform sejt egyetlen akciós potenciállal képes elárasztani GABA-val az axonfelhőjébe nyúló neuron és asztrocita nyúlványokat, melynek hatására klorid ionok áramlanak az asztrocitákból a neuronokba, és kálium ionok áramlanak a neuronokból az asztrocitákba az extracelluláris téren keresztül, mely folyamatok eredményeképpen a neuronális membránok gátlás alá kerülnek úgy, hogy eközben az extracelluláris tér ionikus összetétele a lehető legkisebb mértékben változzon.

Doktori munkám második felében a rágcsáló és emberi agykéreg szupragranuláris rétegeiben található serkentő piramis sejtek szinaptikus kimenetét vizsgáltuk a leggyakoribb helyi gátló sejttípusra, a gyorsan tüzelő interneuronokra. Kutatócsoportunk a közelmúltban kimutatta, hogy ezek a szinaptikus kapcsolatok rendkívül hatékonyan működnek az emberi agykéregben: egy piramis sejt egyetlen akciós potenciálja képes lehet a környező gyorsan tüzelő interneuronokat nyugalmi membránpotenciáljukról küszöb fölé depolarizálni és akciós potenciálba vinni, míg rágcsálók esetében ugyanezen sejtek csupán küszöb alatti depolarizációt érnek el. Doktori munkám során kvantális analízissel megmutatjuk, hogy patkány és ember

esetében az egyetlen vezikula által kiváltott posztszinaptikus áram hasonló amplitúdójú. Fénymikroszkópos vizsgálattal igazoljuk, hogy kapcsolatonként a szinapszisok száma nem mutat fajfüggést. A látszólagos ellentmondást elektron mikroszkópos kísérleteink oldják fel, melyekből kiderül, hogy a hatékony serkentés arra vezethető vissza, hogy az emberben található szinapszisok preszinaptikus aktív zónái nagyobbak, valamint, hogy az ott található dokkolt vezikulák is nagyobb sűrűségben helyezkednek el. Így, ellenben a rágcsálóban megtalálható hasonló szinapszisokkal, akciós potenciálonként egy adott szinapszisban akár több neurotranszmittert tartalmazó vezikula is ürülhet a szinaptikus résbe.

Összefoglalásként elmondható, hogy az emberi és rágcsáló agykéreg összetett működéséhez a szinaptikus mechanizmusok széles palettája járul hozzá.